Chapter 10
Anisotropies in the Cosmic Microwave Background

Long the realm of armchair philosophers, the study of the origins and evolution of the universe became a physical science with falsifiable theories

Wayne Hu, PhD Thesis

In this chapter we attack the hierarchy of Boltzmann equations that we have found for photons and present an approximate, semi-analytic solution which will allow us to understand the temperature correlation in the CMB sky and its relation with the cosmological parameters. Our scope is to understand the features of the angular, temperature-temperature power spectrum in Fig. 10.1.

Note that in this plot the definition

$$\mathcal{D}_\ell^{TT} \equiv \frac{\ell(\ell+1)C_{TT,\ell}}{2\pi} \,, \tag{10.1}$$

is used. We shall see the reason for the $\ell(\ell+1)$ normalisation, whereas the $C_{TT,\ell}$'s are given in Eq. (7.81) as functions of the multipole moments of the temperature distribution and the primordial power spectrum for scalar perturbations.

In Fig. 10.1 we can also see data points up to $\ell \approx 2500$. What can we say from this number about the angular sensitivity of *Planck*? It can be roughly computed as follows. For a given $\ell_{\rm max}$ how many realisations of $a_{\ell m}$ do we have?

Exercise 10.1 For each ℓ we have $2\ell+1$ possible values of m, thus show that:

$$N_{\ell_{\rm max}} = \sum_{\ell=0}^{\ell_{\rm max}} (2\ell+1) = (\ell_{\rm max}+1)^2 \,. \tag{10.2}$$

O. Piattella, *Lecture Notes in Cosmology*, UNITEXT for Physics,
https://doi.org/10.1007/978-3-319-95570-4_10

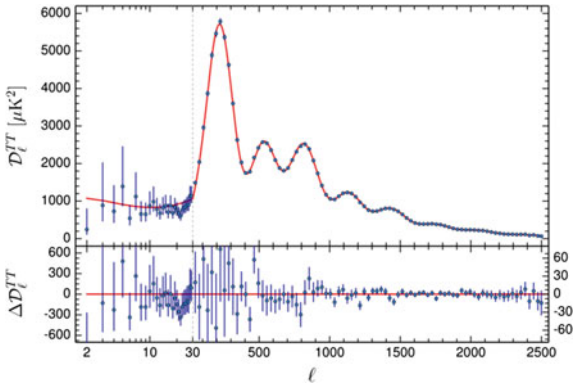

Fig. 10.1 CMB TT spectrum. Figure taken from Ade et al. (2016). The red solid line is the best fit ΛCDM model

The full sky has:

$$4\pi \text{ rad}^2 = \frac{4}{\pi}(180 \text{ deg})^2 \approx 41000 \text{ deg}^2 \, . \tag{10.3}$$

If an experiment has sensitivity of 7 deg, then we can have at most

$$\frac{4}{\pi}(180/7)^2 \approx 842 \, , \tag{10.4}$$

pieces of independent information and therefore we can determine as many $a_{\ell m}$. This gives $\ell_{\rm max} \approx 28$ and it was the sensitivity of *CoBE*. For *Planck*, the angular sensitivity was of 5 arcmin, which corresponds to

$$\frac{4}{\pi}(180 \times 60/5)^2 \approx 10^6 \, , \tag{10.5}$$

pieces of independent information and then to $\ell_{\rm max} = 2436$.

In this chapter we omit the superscript S referring to the scalar perturbations contribution to Θ, since most of the time we shall discuss of it. We shall only use T in order to distinguish the tensor contribution.

10.1 Free-Streaming

It is convenient to start neglecting the collisional term in the Boltzmann equation and considering thus the phase of photon **free-streaming**. The following discussion is similar to the one in Sect. 5.4. Consider Eq. (5.27) for photons and with no collisional term. Using the definition of Θ in Eq. (5.80), we can write for scalar perturbations:

$$\left(\frac{\partial}{\partial\eta}+\frac{dx^i}{d\eta}\frac{\partial}{\partial x^i}\right)(\Theta+\Psi)=\Psi'-\Phi'\ . \tag{10.6}$$

As we know from Boltzmann equation, the differential operator on the left hand side is a convective derivative, i.e. a derivative along the photon path:

$$\frac{d}{d\eta}(\Theta+\Psi)=\Psi'-\Phi'\ , \tag{10.7}$$

whose inversion is the basis of the **line-of-sight integration** approach to CMB anisotropies (Seljak and Zaldarriaga 1996), which is an alternative to attacking the hierarchy of coupled Boltzmann equations (which still must be attacked but can be truncated at much lower ℓ's) as it was done e.g. in Ma and Bertschinger (1995). We shall see this technique in some detail in Sect. 10.5.

For time-independent potentials, as they are in the matter-dominated epoch, the collisionless Boltzmann equation for photons tells us that $\Theta+\Psi$ is constant along the photons paths, i.e. along our past light-cone, since recombination.

Recall that the scalar-perturbed metric that we are using is given in Eq. (4.171):

$$ds^2=-a^2(\eta)(1+2\Psi)d\eta^2+a^2(\eta)(1+2\Phi)\delta_{ij}dx^i dx^j\ . \tag{10.8}$$

Inside a potential well, Ψ is negative. In order to be convinced of this one has just to think about the Newtonian limit and realise that 2Ψ is the Newtonian gravitational potential, hence negative. So, since $\Theta+\Psi$ stays constant, we have that:

$$\Theta(\eta_*,\mathbf{x}_*,\hat{p})+\Psi(\eta_*,\mathbf{x}_*)=\Theta(\eta_0,\mathbf{x}_0,\hat{p})+\Psi(\eta_0,\mathbf{x}_0)\ . \tag{10.9}$$

where on the left hand side we have chosen the quantities at recombination whereas on the right hand side we have chosen the present time. Note that $\mathbf{x}_0$, is where our laboratory (the CMB experiment) is, i.e. Earth, and as such is fixed. Therefore, since we can only detect photons on our past light-cone, and those from CMB comes from a fixed comoving distance $r_*=\eta_0-\eta_*$, we have that:

$$\mathbf{x}_*=\mathbf{x}_0-r_*\hat{p}\ . \tag{10.10}$$

Note that $\hat{p}$ is the photon direction and so it is opposite to the direction of the line of sight $\hat{n}=-\hat{p}$. So, the only independent variables are 2, the components of $\hat{p}$. They become just a single one, μ, because of the way in which we factorise the azimuthal dependence (and assuming axial symmetry).

The potential $\Psi(\eta_0,\mathbf{x}_0)$ is usually neglected, or incorporated in the potential at recombination, since it is not detectable. As it is well known, classically only potential differences are physically meaningful. The above equation then tells us that:

$$\Theta(\eta_*,\mathbf{x}_0-r_*\hat{p},\hat{p})+\Psi(\eta_*,\mathbf{x}_0-r_*\hat{p})=\Theta(\eta_0,\mathbf{x}_0,\hat{p})\ , \tag{10.11}$$

i.e. the observed temperature fluctuation (on the right hand side) accounts for the energy loss due to climbing out the potential well or falling down a potential hill. This is the so-called **Sachs-Wolfe effect** (Sachs and Wolfe 1967). Writing the above equation in Fourier modes, we have:

$$\int \frac{d^3\mathbf{k}}{(2\pi)^3}\Theta(\eta_0,\mathbf{k},\hat{p})e^{i\mathbf{k}\cdot\mathbf{x}_0} = \int \frac{d^3\mathbf{k}}{(2\pi)^3}\left[\Theta(\eta_*,\mathbf{k},\hat{p})+\Psi(\eta_*,\mathbf{k})\right]e^{i\mathbf{k}\cdot(\mathbf{x}_0-r_*\hat{p})}\,. \tag{10.12}$$

We can set now $\mathbf{x}_0 = 0$, without losing of generality, and manifest the dependences as k and μ, the former since we normalise to the scalar primordial mode $\alpha(\mathbf{k})$, cf. Eq. (7.64), and the latter since we are considering axisymmetric scalar perturbations. Hence we have for the Fourier modes:

$$\Theta(\eta_0,k,\mu) = \left[\Theta(\eta_*,k,\mu)+\Psi(\eta_*,k)\right]e^{-ik\mu r_*}\,. \tag{10.13}$$

Using the partial wave expansion, we get:

$$\Theta_\ell(\eta_0,k) = \frac{1}{(-i)^\ell}\int_{-1}^{1}\frac{d\mu}{2}\mathcal{P}_\ell(\mu)\left[\Theta(\eta_*,k,\mu)+\Psi(\eta_*,k)\right]e^{-ik\mu r_*}\,, \tag{10.14}$$

and using the relation:

$$\int_{-1}^{1}\frac{d\mu}{2}\,\mathcal{P}_\ell(\mu)e^{-ik\mu r_*} = (-i)^\ell j_\ell\left(kr_*\right)\,, \tag{10.15}$$

which can be obtained by inverting the expansion of Eq. (5.75), we can write:

$$\Theta_\ell(\eta_0,k) = \Psi(\eta_*,k)\,j_\ell(kr_*) + \frac{1}{(-i)^\ell}\int_{-1}^{1}\frac{d\mu}{2}\mathcal{P}_\ell(\mu)\Theta(\eta_*,k,\mu)e^{-ik\mu r_*}\,. \tag{10.16}$$

Using again the partial wave expansion, we can write the above formula as:

$$\Theta_\ell(\eta_0,k) = \Psi(\eta_*,k)\,j_\ell(kr_*) + \frac{1}{(-i)^\ell}\sum_{\ell'}(-i)^{\ell'}(2\ell'+1)\Theta_{\ell'}(\eta_*,k)\int_{-1}^{1}\frac{d\mu}{2}\mathcal{P}_\ell(\mu)\mathcal{P}_{\ell'}(\mu)e^{-ik\mu r_*}\,. \tag{10.17}$$

We shall see later that, because of tight-coupling, the monopole and the dipole contribute the most at recombination. Hence, we can write, truncating the summation at $\ell' = 1$:

$$\Theta_\ell(\eta_0,k) = \left(\Theta_0+\Psi\right)(\eta_*,k)\,j_\ell(kr_*) + \frac{3\Theta_1(\eta_*,k)}{(-i)^{\ell-1}}\int_{-1}^{1}\frac{d\mu}{2}\mathcal{P}_\ell(\mu)\mu e^{-ik\mu r_*}\,. \tag{10.18}$$

The integral can be performed as follows:

$$\int_{-1}^{1} \frac{d\mu}{2} \mathcal{P}_\ell(\mu) \mu e^{-ik\mu r_*} = i \frac{d}{d(kr_*)} \int_{-1}^{1} \frac{d\mu}{2} \mathcal{P}_\ell(\mu) e^{-ik\mu r_*} = \frac{1}{i^{\ell-1}} \frac{d}{d(kr_*)} j_\ell(kr_*) \ . \tag{10.19}$$

The same technique can be used, in principle, to calculate the integral for any ℓ': for each power of μ one gains a derivative of the spherical Bessel function. Recalling the formula (Abramowitz and Stegun 1972)[1]:

$$\frac{dj_\ell(x)}{dx} = j_{\ell-1}(x) - \frac{\ell+1}{x} j_\ell(x) \ , \tag{10.20}$$

we can write:

$$\begin{aligned} \Theta_\ell(\eta_0, k) &= (\Theta_0 + \Psi)(\eta_*, k) j_\ell(kr_*) \\ &+ 3\Theta_1(\eta_*, k) \left[j_{\ell-1}(kr_*) - \frac{\ell+1}{kr_*} j_\ell(kr_*) \right] . \end{aligned} \tag{10.21}$$

So, the spherical Bessel functions that we have mentioned in Chap. 9 start to appear. We have obtained the above free-streaming solution neglecting the potentials derivatives in Eq. (10.7). Taking them into account is not difficult, since an additional piece containing the integration of the potential derivatives would appear in Eq. (10.13):

$$\Theta(\eta_0, k, \mu) = [\Theta(\eta_*, k, \mu) + \Psi(\eta_*, k)] e^{-ik\mu r_*} + \int_{\eta_*}^{\eta_0} d\eta \, (\Psi' - \Phi')(\eta, k) e^{-ik\mu(\eta_0 - \eta)} \ . \tag{10.22}$$

The exponential factor in the integral comes from the Fourier transform of the potentials and from considering:

$$\mathbf{x} = \mathbf{x}_0 - (\eta_0 - \eta)\hat{p} \ , \tag{10.23}$$

at any given time η along the photon trajectory (this is the "line of sight", in practice). Performing again the expansion in partial waves, we get:

$$\begin{aligned} \Theta_\ell(\eta_0, k) &= (\Theta_0 + \Psi)(\eta_*, k) j_\ell(kr_*) \\ &+ 3\Theta_1(\eta_*, k) \left[j_{\ell-1}(kr_*) - \frac{\ell+1}{kr_*} j_\ell(kr_*) \right] \\ &+ \int_{\eta_*}^{\eta_0} d\eta \, [\Psi'(\eta, k) - \Phi'(\eta, k)] j_\ell(kr) \ , \end{aligned} \tag{10.24}$$

where

$$r \equiv \eta_0 - \eta \ . \tag{10.25}$$

As we are going to see, the first two terms of the above formula contains the **primary anisotropies** of the CMB, which are the **acoustic oscillations** and the **Doppler effect**. The $\Psi(\eta_*, k)$ contribution in the first term is, as we have already anticipated,

[1] The website http://functions.wolfram.com is also very useful.

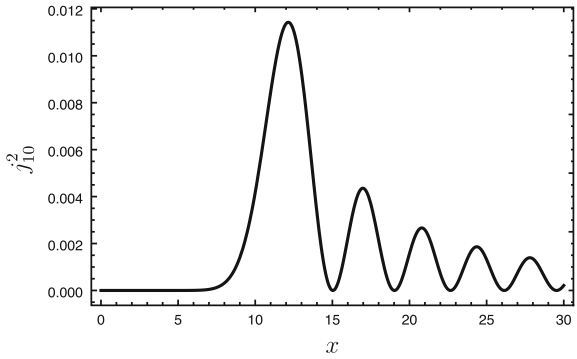

Fig. 10.2 Evolution of the spherical Bessel function $j_{10}^2(x)$

the **Sachs-Wolfe effect**. The last term is the **Integrated Sachs-Wolfe** (ISW) effect (Sachs and Wolfe 1967) and contributes only when the gravitational potentials are time-varying. This happens, as we have seen in Chap. 9, when radiation and DE are relevant. For this reason the ISW effect is usually separated in the early-times one, due to a small presence of radiation still at decoupling, and in the late-times one, due to DE.

Once we know all the contributions of the above formula, we can use Eq. (7.81) and provide the prediction on the $C^S_{TT,\ell}$ spectrum.

The presence of the spherical Bessel function is interesting for two reasons, which we display in Fig. 10.2 for the arbitrary choice $\ell = 10$.

We have chosen to plot the squared spherical Bessel function because it is the relevant window function when computing the C_ℓ's, as we shall see briefly. First, the maximum value is attained roughly when $x \approx \ell$ and for $x < \ell$ the spherical Bessel function is practically vanishing. Therefore, for a given multipole ℓ the scale which contribute most for the observed anisotropy is:

$$k \approx \frac{\ell}{\eta_0 - \eta_*} \,. \tag{10.26}$$

We have anticipated this already in Chap. 9. The second reason of interest is that the spherical Bessel function goes to zero for large x. This means that scales such that $kr_* \gg 1$ do not contribute to the observed anisotropy. Physically, this is an effect due to the free-streaming phase for which, on very small scales, hot and cold photons mix up destroying thus the anisotropy.

We have thus seen that the predicted anisotropy today is given by formula Eq. (10.24). We have now to justify the fact of considering only the monopole and the dipole at recombination. We shall commence in the next section discussing very large scales.

In principle, Eq. (10.24) has the very same form for neutrinos, but with an initial conformal time η_i which is well anterior to η_*, since neutrinos do not interact and therefore they only free-stream (at least for temperatures of the primordial plasma below 1 MeV).

10.2 Anisotropies on Large Scales

On large scales, i.e. $k\eta \ll 1$, the relevant equations are those of Chap. 6, which we report here:

$$\delta'_\gamma = -4\Phi' \,, \quad \delta'_\nu = -4\Phi' \,, \quad \delta'_{\rm c} = -3\Phi' \,, \quad \delta'_{\rm b} = -3\Phi' \,, \tag{10.27}$$

i.e. only the monopoles are relevant. Since we want to describe CMB, let us focus on the photon density contrast, which can be written as:

$$\delta_\gamma(k,\eta) = 4\Theta_0(k,\eta) \,, \tag{10.28}$$

introducing the monopole of the temperature fluctuation. The equation $\Theta'_0 = -\Phi'$ can be immediately integrated, obtaining:

$$\Theta_0(k,\eta) = -\Phi(k,\eta) + C_\gamma(k) \,. \tag{10.29}$$

For the adiabatic primordial mode, the only which we are going to consider, we know from Eq. (6.94) that $C_\gamma(k) = \Phi_{\rm P}(k) - \Psi_{\rm P}(k)/2$ and thus:

$$\Theta_0(k,\eta) = -\Phi(k,\eta) + \Phi_{\rm P}(k) - \frac{1}{2}\Psi_{\rm P}(k) \,. \tag{10.30}$$

As we know from Chap. 9, we can consider the gravitational potentials to be equal in modulus and on large scales $\Phi(k,\eta)$ is independent of time and since recombination $\eta_* \gg \eta_{\rm eq}$ takes place well after radiation-matter equality, we know that $\Phi(k,\eta_*) = 9\Phi_{\rm P}(k)/10$, i.e. the value of the gravitational potential drops of 10% in passing through radiation-matter domination. Therefore:

$$\Theta_0(k,\eta_*) = \frac{3}{5}\Phi_{\rm P}(k) = \frac{2}{3}\Phi(k,\eta_*) = -\frac{2}{3}\Psi(k,\eta_*) \,. \tag{10.31}$$

As we saw earlier in Eq. (10.24), the observed anisotropy is not $\Theta_0(k,\eta_*)$ but $\Theta_0(k,\eta_*) + \Psi(k,\eta_*)$, because of the gravitational redshift. Again, this is the Sachs-Wolfe effect, amounting to a shift in the photons frequency when they decouple from the baryonic plasma depending whether they are in a well or hill of the gravitational potential. So, we have from Eq. (10.31) that:

$$(\Theta_0 + \Psi)(k,\eta_*) = \frac{1}{3}\Psi(k,\eta_*) \,. \tag{10.32}$$

On the other hand, for $\delta_{\rm c}$ we know that

$$\delta_{\rm c}(k,\eta) = -3\Phi(k,\eta) + \frac{9\Phi_{\rm P}(k)}{2} \,, \tag{10.33}$$

again assuming adiabatic primordial modes. Using again $\Phi(k,\eta_*) = 9\Phi_{\rm P}(k)/10$, we get:

$$\delta_{\rm c}(k,\eta_*) = 2\Phi(k,\eta_*) = -2\Psi(k,\eta_*)\ . \tag{10.34}$$

The fluctuations in CDM contribute more in generating the potential wells than photons, a factor 2 against a factor $-2/3$. Combining the two equations:

$$\boxed{(\Theta_0+\Psi)(k,\eta_*) = -\frac{\delta_{\rm c}(k,\eta_*)}{6}} \tag{10.35}$$

This result tells us that on large scales colder spots represent larger overdensities, a counter-intuitive result. One expects hotter photons the deeper the well is and in fact this is the case with just $\Theta_0(k,\eta_*)$, since we have:

$$\Theta_0(k,\eta_*) = -\frac{2}{3}\Psi(k,\eta_*) = \frac{\delta_{\rm c}(k,\eta_*)}{3}\ , \tag{10.36}$$

i.e. the larger the CDM overdensity, the larger the well and $\Theta_0(k,\eta_*)$ are. However, photons' response to the gravitational potential is only a factor $-2/3$ whereas the gravitational redshift adds a Ψ contribution, changing thus the sign of the observed anisotropy. In the limit of $\delta_{\rm c} \to -1$, one gets $(\Theta_0+\Psi)(k,\eta_*) \to 1/6$, so cosmic voids correspond to hot spots!

The results found here are valid only on large scales, i.e. for $k\eta_* \ll 1$, scales much larger than the horizon at recombination, which has an angular size of approximatively 1 degree. Moreover, they also depend on the choice of initial conditions. We have opted for the adiabatic ones, as usual.

Exercise 10.2 Reproduce the above argument for the other primordial modes.

Let us use the theoretical prediction on the $C^S_{TT,\ell}$ given in Eq. (7.81) together with the first contribution only from Eq. (10.24). The latter approximation is justified by the fact that we are considering large scales, hence the dipole contribution is negligible and the ISW effect is vanishing because the potentials are constant. Since:

$$(\Theta_0+\Psi)(k,\eta_*) = \frac{1}{3}\Psi(k,\eta_*) = -\frac{1}{3}\Phi(k,\eta_*) = -\frac{3}{10}\Phi_{\rm P}(k) = -\frac{1}{5}\mathcal{R}(k)\ , \tag{10.37}$$

the transfer function is just the constant $-1/5$ (recall that we are neglecting the neutrino fraction R_ν) and thus the angular power spectrum is:

$$C^S_{TT,\ell}({\rm SW}) = \frac{4\pi}{25}\int_0^\infty \frac{dk}{k}\Delta^2_{\mathcal{R}}(k)\, j^2_\ell(k\eta_0)\ , \tag{10.38}$$

since $\eta_* \ll \eta_0$. Note that $k\eta_* \ll k\eta_0$ and we have seen in Fig. 10.2 that the spherical Bessel function contributes the most about $k\eta_0 \approx \ell$. Thus, for small ℓ, i.e. large angular scales, $k\eta_0$ is small and $k\eta_*$ is very small, where in fact $|\,(\Theta_0 + \Psi)\,(k, \eta_*)|^2$ is constant. In other words, the above approximation is valid for small ℓ, typically $\ell \lesssim 30$.

In the above integral we can look at $j_\ell^2(k\eta_0)$ as a very peaked window function and approximate it as:

$$C_{TT,\ell}^S(\mathrm{SW}) \approx \frac{4\pi}{25}\Delta_{\mathcal{R}}^2(\ell/\eta_0)\int_0^\infty \frac{dk}{k}\, j_\ell^2(k\eta_0)\ . \tag{10.39}$$

Using the result:

$$\int_0^\infty \frac{dx}{x}\, j_\ell^2(x) = \frac{1}{2\ell(\ell+1)}\ , \tag{10.40}$$

we have then:

$$\frac{\ell(\ell+1)C_{TT,\ell}^S(\mathrm{SW})}{2\pi} \approx \frac{1}{25}\Delta_{\mathcal{R}}^2(\ell/\eta_0)\ . \tag{10.41}$$

Hence, for a scale-invariant spectrum $n_S = 1$ the combination $\ell(\ell+1)C_{TT,\ell}^S(\mathrm{SW})$ is constant and it is called **Sachs-Wolfe plateau**. This also explains why CMB power spectra are usually presented with the $\ell(\ell+1)$ normalisation, as in Fig. 10.1.

If $n_S \neq 1$, then $\ell(\ell+1)C_{TT,\ell}^S(\mathrm{SW})$ is proportional to ℓ^{n_S-1}, i.e. the **primordial tilt** in the power spectrum leaves its mark in a tilted plateau for small ℓ.

10.3 Tight-Coupling and Acoustic Oscillations

We have seen that in order to determine the prediction on the present time $C_{TT,\ell}$'s we need to know what happens at recombination. We devote this section to such purpose, showing that the monopole and the dipole contribute the most.

Let us recover here the hierarchy of Boltzmann equations for the Θ_ℓ's (not taking into account polarisation) that we have derived in Chap. 5:

$$(2\ell+1)\Theta_\ell' + k[(\ell+1)\Theta_{\ell+1} - \ell\Theta_{\ell-1}] = (2\ell+1)\tau'\Theta_\ell\ , \qquad (\ell > 2)\ , \tag{10.42}$$

$$10\Theta_2' + 2k\,(3\Theta_3 - 2\Theta_1) = 10\tau'\Theta_2 - \tau'\Pi\ , \tag{10.43}$$

$$3\Theta_1' + k(2\Theta_2 - \Theta_0) = k\Psi + \tau'\,(3\Theta_1 - V_{\mathrm{b}})\ , \tag{10.44}$$

$$\Theta_0' + k\Theta_1 = -\Phi'\ , \tag{10.45}$$

where recall that $\delta_\gamma = 4\Theta_0$ and $3\Theta_1 = V_\gamma$. The best way to deal with these equations is to solve them numerically by using Boltzmann codes such as CAMB or CLASS, but in this way the physics behind the $C_{TT,\ell}$'s remains hidden or unclear. For this reason we attack these equations in an approximate fashion, but analytically.

We take the limit $-\tau' \gg \mathcal{H}$, which is called **tight-coupling** (TC) approximation. This limit physically means that the Thomson scattering rate between photons and electrons is much larger than the Hubble rate until recombination and then drops abruptly since the free electron fraction X_e goes to zero very rapidly, as we have seen when studying thermal history in Chap. 3. We shall first consider the case of **sudden recombination**, where all the photons last scatter at the same time. It is a fair approximation, though unrealistic.

Exercise 10.3 From the definition of the optical depth:

$$\tau \equiv \int_{\eta}^{\eta_0} d\eta' \, n_e \sigma_{\rm T} a \ , \tag{10.46}$$

show that $\tau \propto 1/\eta^3$ when matter dominates and $\tau \propto 1/\eta$ when radiation dominates.

We can be more quantitative and write:

$$-\tau' = n_e \sigma_{\rm T} a = n_{\rm b} \sigma_{\rm T} a = \frac{\rho_{\rm b}}{m_{\rm b}} \sigma_{\rm T} a \ , \tag{10.47}$$

where we have used the definition of τ and assumed to be in an epoch before recombination, so that we can approximate n_e with $n_{\rm b}$, since all the electrons are free.

Exercise 10.4 Introducing the baryon density parameter and using $m_{\rm b} = 1$ GeV, the mass of the proton, show that:

$$-\tau' \approx 1.46 \times 10^{-19} \frac{\Omega_{\rm b0} h^2}{a^2} \ {\rm s}^{-1} \ . \tag{10.48}$$

Now we need to compare this scattering rate with the Hubble rate, in order to check the goodness of the TC approximation. Assuming matter-domination and using the conformal time Friedmann equation (this because τ' is derived with respect to the conformal time), we have:

$$\mathcal{H} = H_0 \sqrt{\Omega_{\rm m0}} a^{-1/2} \approx 3.33 \times 10^{-18} h \sqrt{\Omega_{\rm m0}} \, a^{-1/2} \ {\rm s}^{-1} \ . \tag{10.49}$$

Therefore, the ratio:

$$\frac{-\tau'}{\mathcal{H}} = 0.044 \, \frac{\Omega_{\rm b0} h^2}{\sqrt{\Omega_{\rm m0} h^2}} a^{-3/2} \ , \tag{10.50}$$

diverges for $a \to 0$ as expected (though the formula should be generalised to the case of radiation-domination), so if it is sufficiently big at recombination then the

TC approximation would be reliable. Substituting the *Planck* values $\Omega_{\rm b0}h^2 = 0.022$ and $\Omega_{\rm m0}h^2 = 0.12$ one gets at recombination, i.e. for $a = 10^{-3}$:

$$\frac{-\tau'}{\mathcal{H}} \approx 10^2 \ . \tag{10.51}$$

This means that the scattering rate is much larger than the Hubble rate even at recombination as long as there are free electrons around and thus we are going to use the tight-coupling approximation with reliability.

Let us see in detail how the TC limit works. Let us compare in the hierarchy for $\ell \geq 2$ the terms Θ'_ℓ and $k\Theta_\ell$ with $\tau'\Theta_\ell$, which have all the same dimensions of inverse time. There are two physical time scales in our problem, one is given by the expansion rate and the other by the scattering rate, hence

$$\Theta'_\ell \propto \mathcal{H}\Theta_\ell, \tau'\Theta_\ell \ , \tag{10.52}$$

from a dimensional analysis. However, the mode for which $\Theta'_\ell \propto \tau'\Theta_\ell$ implies that $\Theta_\ell \propto \exp\tau$ and hence diverges at early times, which is unacceptable for a small fluctuation. We then dismiss this mode as unphysical and take into account just that for which $\Theta'_\ell \propto \mathcal{H}\Theta_\ell$, which is small compared to $\tau'\Theta_\ell$.

Now, let us inspect the ratio

$$\frac{-\tau'}{k} \ . \tag{10.53}$$

This is the number of collisions which take place on a scale $1/k$. Hence, this number is very large, provided that we consider sufficiently large scales, i.e. small k. If the scale is too small, i.e. large k, then the TC approximation does not work well and we must take into account the multipole moments for $\ell \geq 2$. We will see this when investigating the **diffusion damping** or **Silk damping** effect.

From the above analysis, for sufficiently large scales we can conclude then that $\Theta_\ell \approx 0$ for $\ell \geq 2$. Sufficiently large means much larger than the mean free path $-1/\tau'$ which is approximately of the order of 10 Mpc at recombination. This number can be computed from Eq. (10.48) and is a comoving scale; the physical one is divided by a factor a thousand and so it is 10 kpc.

Finally, note that $\Theta_\ell \sim \tau'/k\Theta_{\ell-1}$. Therefore, considering smaller and smaller scales makes necessary to include higher and higher order multipoles.

Eliminating all the multipoles $\ell \geq 2$, the relevant equations are just the following two:

$$\Theta'_0 + k\Theta_1 = -\Phi' \ , \tag{10.54}$$

$$3\Theta'_1 - k\Theta_0 = k\Psi + \tau'\,(3\Theta_1 - V_{\rm b}) \ , \tag{10.55}$$

i.e. the TC approximation allows us to treat photons as a fluid until recombination. Note the coupling to baryons via the baryon velocity $V_{\rm b}$. Thus, we need also the equations for baryons:

$$\delta_{\rm b}' + kV_{\rm b} = -3\Phi' \,, \tag{10.56}$$

$$V_{\rm b}' + \mathcal{H}V_{\rm b} = k\Psi + \frac{\tau'}{R}(V_{\rm b} - 3\Theta_1) \,, \tag{10.57}$$

where we have introduced $R \equiv 3\rho_{\rm b}/4\rho_\gamma$, i.e. the baryon density to photon density ratio. This number can be cast as:

$$R = \frac{3\Omega_{\rm b0}}{4\Omega_{\gamma 0}} a \approx 600a \,, \tag{10.58}$$

using the usual values and it grows from zero at early times to $R_* \approx 0.6$ at recombination. So it is small, but not that negligible. Let us rewrite the velocity equation for baryons in the following way:

$$V_{\rm b} = 3\Theta_1 + \frac{R}{\tau'}\left(V_{\rm b}' + \mathcal{H}V_{\rm b} - k\Psi\right) \,. \tag{10.59}$$

We can solve this equation via successive approximation, exploiting the fact that $R < 1$ before recombination. That is, assume the expansion:

$$V_{\rm b} = V_{\rm b}^{(0)} + RV_{\rm b}^{(1)} + R^2 V_{\rm b}^{(2)} + \cdots \,. \tag{10.60}$$

The solution for $R = 0$ simply gives $V_{\rm b}^{(0)} = 3\Theta_1$, which we have used in Chap. 6 in order to investigate the primordial modes. This solution is reliable well before recombination, say at $a = 10^{-7}$ for example, because $R \approx 6 \times 10^{-5}$ there, but it is not satisfactory at recombination and we shall take into account the first order in R in the above expansion.

10.3.1 The Acoustic Peaks for $R = 0$

Let us start with the simple case of $R = 0$, which amounts to neglect baryons.

Exercise 10.5 Combine the photon Eqs. (10.54)–(10.55) with the zeroth-order TC condition $V_{\rm b} = 3\Theta_1$ and find the following second-order equation for Θ_0:

$$\Theta_0'' + \frac{k^2}{3}\Theta_0 = -\frac{k^2\Psi}{3} - \Phi'' \,. \tag{10.61}$$

We have here already the first fundamental piece of physics of the CMB. This is the equation of motion of a driven harmonic oscillator where instead of the position we have the monopole of the temperature fluctuation and the driving force is given by the gravitational potential. This equation describe **acoustic oscillations** of the

baryon-photon fluid until recombination. After recombination we expect to observe these fluctuations in the $C_{TT,\ell}$'s, using the free-streaming formula (10.24), and in fact we do, cf. Fig. 10.1.

Note that these oscillations are in the baryon-photon fluid and therefore affect also baryons. We therefore expect to see oscillations in the baryon distribution after recombination, called **baryon acoustic oscillations** (BAO), and detected by Eisenstein and collaborators in 2005 (Eisenstein et al. 2005). The BAO are the manifestation of a special length, the sound horizon at recombination, in the correlation function of galaxies which appears as a bump, i.e. an excess probability. In the Fourier space, i.e. for the power spectrum, a given scale is represented with various oscillations. We have already encountered BAO in Chap. 9. BAO and weak gravitational lensing are among the main observables on which current and future experiments (such as *Euclid* and *LSST*) are based.

Exercise 10.6 Combine Eqs. (10.56) and (10.57) and the TC condition $V_\mathrm{b} = 3\Theta_1$ and find the following equation for δ_b:

$$\delta_\mathrm{b}' = 3\Theta_0' \,. \tag{10.62}$$

Hence, the same oscillatory solution of Θ_0 holds true for δ_b.

Now, consider the fact that close to recombination CDM is already dominating and thus the potentials are equal and constant at all scales. We get:

$$\Theta_0'' + \frac{k^2}{3}\Theta_0 = -\frac{k^2\Psi}{3} \,. \tag{10.63}$$

This equation can be put in the following form:

$$(\Theta_0 + \Psi)'' + \frac{k^2}{3}(\Theta_0 + \Psi) = 0 \,, \tag{10.64}$$

where we have used the constancy of Ψ. Note how the observed temperature fluctuation, used in Eq. (10.24), has appeared. The solution is:

$$(\Theta_0 + \Psi)(\eta, k) = A(k)\sin\left(\frac{k\eta}{\sqrt{3}}\right) + B(k)\cos\left(\frac{k\eta}{\sqrt{3}}\right) \,, \tag{10.65}$$

with the driving potential, i.e. CDM, providing just an offset for the oscillations. At recombination we have

$$(\Theta_0 + \Psi)(\eta_*, k) = A(k)\sin\left(\frac{k\eta_*}{\sqrt{3}}\right) + B(k)\cos\left(\frac{k\eta_*}{\sqrt{3}}\right) \,, \tag{10.66}$$

with peaks and valleys in the temperature fluctuations given by this combination of sine and cosine, therefore dependent on the functions $A(k)$ and $B(k)$. Inserting these formula into Eq. (10.24) in order to compute the $\Theta_\ell(\eta_0, k)$ (the anisotropies today) and then into Eq. (7.81) in order to compute the $C_{TT,\ell}$'s, we are able to explain the **acoustic oscillations** feature of the CMB TT spectrum, of Fig. 10.1.

The functions $A(k)$ and $B(k)$ are determined by the initial condition, i.e. for $k\eta_* \ll 1$:

$$(\Theta_0 + \Psi)(k\eta_* \ll 1) \sim A(k)\frac{k\eta_*}{\sqrt{3}} + B(k) \ . \tag{10.67}$$

Hence, if we choose adiabatic modes, we must put $A(k) = 0$. So, considering different initial conditions changes the position of the acoustic peaks and observation allows to test the choice made. As we saw in Chap. 6, Planck limits the presence of isocurvature modes to a few percent. With $A(k) = 0$, i.e. for adiabatic perturbations, using the large-scale solution that we found in Eq. (10.37), we have:

$$(\Theta_0 + \Psi)(\eta_*, k) = -\frac{1}{5}\mathcal{R}(k)T(k)\cos\left(\frac{k\eta_*}{\sqrt{3}}\right) \ , \tag{10.68}$$

where $T(k)$ is the transfer function of $\Theta_0 + \Psi$. We did not calculate it in Chap. 9, but it can be shown that it is limited to a range 0.4-2, approximately. See Mukhanov (2005).

The extrema of the effective temperature fluctuations are thus given by:

$$\frac{k\eta_*}{\sqrt{3}} = n\pi \ , \qquad (n = 1, 2, \dots) \ , \tag{10.69}$$

where the odd values provide peaks, corresponding to the highest temperature fluctuations and thus to scales at which photons are maximally compressed and hot, whereas the even values provide throats, corresponding to the lowest temperature fluctuations and thus to scales at which photons are maximally rarefied and cold. In the spectrum, cf. Fig. 10.1, only peaks appear because of the quadratic nature of the $C_{TT,\ell}$'s as functions of the Θ_ℓ's, but it should be clear that the first and the third peaks are compressional.

From Eqs. (10.54) and (10.68), we can determine easily the dipole contribution:

$$\Theta_1(\eta_*, k) = -\frac{\Theta_0'(\eta_*, k)}{k} = -\frac{1}{5\sqrt{3}}\mathcal{R}(k)T(k)\sin\left(\frac{k\eta_*}{\sqrt{3}}\right) \ , \tag{10.70}$$

where we are still continuing in keeping the potentials constant. Substituting this equation and Eq. (10.68) into Eq. (10.24) and then into Eq. (7.81) in order to compute the angular power spectrum, we get:

$$C_{TT,\ell} = \frac{4\pi}{25}\int_0^\infty \frac{dk}{k}\Delta^2_{\mathcal{R}}(k)\left[\cos\left(\frac{k\eta_*}{\sqrt{3}}\right) j_\ell(k\eta_0) + \sqrt{3}\sin\left(\frac{k\eta_*}{\sqrt{3}}\right)\frac{dj_\ell(k\eta_0)}{d(k\eta_0)}\right]^2 , \tag{10.71}$$

where the derivative of the spherical Bessel function is given in Eq. (10.20). We have put $T(k) = 1$ here for simplicity.

We can manipulate analytically this integral following the technique used in Mukhanov (2004, 2005). In these references, baryon loading and diffusion damping are taken into account but here we just tackle a simpler case.

The idea is to avoid the oscillatory nature of the Bessel function and of the trigonometric ones (which are also problematic from a numerical perspective) by approximating $j_\ell(x)$ as follows, for large ℓ:

$$j_\ell(x) \approx \begin{cases} 0\,, & (x < \ell)\,, \\ \frac{1}{\sqrt{x}(x^2-\ell^2)^{1/4}}\cos\left[\sqrt{x^2-\ell^2} - \ell\arccos(\ell/x) - \pi/4\right], & (x > \ell)\,. \end{cases} \tag{10.72}$$

This approximation is identical either for $j_\ell(x)$ and for $j_{\ell-1}(x)$, since we are assuming ℓ to be large. Hence, when we deal with the derivative of the spherical Bessel function in Eq. (10.71), we can factorise a $j^2_\ell(x)$ and we can approximate the squared cosine coming from the above approximation with its average, i.e. a factor $1/2$. We thus have the following integration:

$$C_{TT,\ell} = \frac{2\pi\Delta^2_{\mathcal{R}}}{25}\int_{\ell/\eta_0}^\infty \frac{dk}{k^2\eta_0\sqrt{(k\eta_0)^2-\ell^2}}\left[\cos\left(\frac{k\eta_*}{\sqrt{3}}\right) + \sqrt{3}\left(1-\frac{\ell}{k\eta_0}\right)\sin\left(\frac{k\eta_*}{\sqrt{3}}\right)\right]^2 , \tag{10.73}$$

where we have already assumed a scale-invariant spectrum, for simplicity. Using now the variable

$$x \equiv \frac{k\eta_0}{\ell}\,, \tag{10.74}$$

we can write:

$$\ell^2 C_{TT,\ell} = \frac{2\pi\Delta^2_{\mathcal{R}}}{25}\int_1^\infty \frac{dx}{x^2\sqrt{x^2-1}}\left[\cos(\ell\varrho x) + \sqrt{3}\frac{x-1}{x}\sin(\ell\varrho x)\right]^2 , \tag{10.75}$$

where note the appearance of the factor ℓ^2 on the left hand side and we have defined the quantity:

$$\varrho \equiv \frac{\eta_*}{\sqrt{3}\eta_0}\,. \tag{10.76}$$

Now, developing the square and using the trigonometric formulae:

$$\cos^2\alpha = \frac{1+\cos 2\alpha}{2}\,, \qquad \sin^2\alpha = \frac{1-\cos 2\alpha}{2}\,, \qquad 2\sin\alpha\cos\alpha = \sin 2\alpha\,, \tag{10.77}$$

we can write:

$$\ell^2 C_{TT,\ell} = \frac{2\pi\Delta^2_{\mathcal{R}}(k)}{25}\int_1^\infty \frac{dx}{x^2\sqrt{x^2-1}} \left[\frac{x^2+3(x-1)^2}{2x^2} + \frac{x^2-3(x-1)^2}{2x^2}\cos(2\ell\varrho x) + \frac{\sqrt{3}(x-1)}{x}\sin(2\ell\varrho x)\right] . \tag{10.78}$$

Now, let us treat separately the three integrands. The first, non-oscillatory one is simplest one:

$$N \equiv \int_1^\infty \frac{dx}{x^2\sqrt{x^2-1}}\frac{x^2+3(x-1)^2}{2x^2} = 3\left(1-\frac{\pi}{4}\right) , \tag{10.79}$$

but also the less interesting. The oscillatory ones can be dealt with following Mukhanov (2005). Define:

$$O_1 \equiv \int_1^\infty \frac{dx}{\sqrt{x-1}}\frac{x^2-3(x-1)^2}{2x^4\sqrt{x+1}}\cos(2\ell\varrho x) , \tag{10.80}$$

then solving the problem in Mukhanov (2005, p. 383), we can use the formula:

$$\int_1^\infty \frac{dx}{\sqrt{x-1}} f(x)\cos(bx) \approx f(1)\sqrt{\frac{\pi}{b}}\cos(b+\pi/4) , \tag{10.81}$$

for large values of b and a slowly varying $f(x)$. A similar result holds true also for the sine function. Using this formula we have then:

$$O_1 = \frac{1}{2\sqrt{2}}\sqrt{\frac{\pi}{2\ell\varrho}}\cos(2\ell\varrho+\pi/4) , \tag{10.82}$$

whereas for the integral containing the sine:

$$O_2 \equiv \int_1^\infty \frac{dx}{\sqrt{x-1}}\frac{\sqrt{3}(x-1)}{x^3\sqrt{x+1}}\sin(2\ell\varrho x) \approx 0 , \tag{10.83}$$

since $f(1) = 0$ here. The contribution O_2 comes from the cross product between the monopole and the dipole terms and it is usually neglected in the calculations. We have explicitly shown why here. Gathering the N and O_1 contributions, we plot the sum $N + O_1$ in Fig. 10.3.

In order to make this plot, we have used $a \propto \eta^2$, since we are in the matter-dominated epoch, and thus we have evaluated ϱ as follows:

$$\varrho = \frac{\eta_*}{\sqrt{3}\eta_0} = \frac{1}{\sqrt{3(1+z_*)}} = \frac{1}{\sqrt{3000}} \approx 0.0183 . \tag{10.84}$$

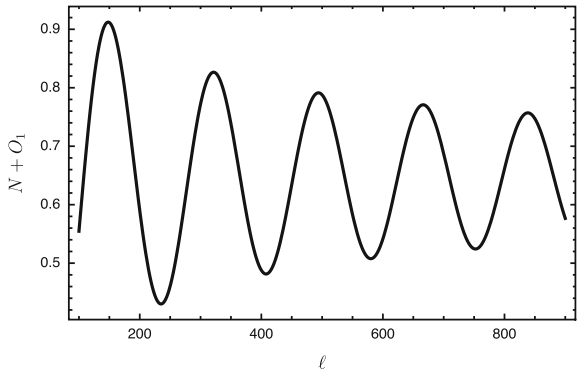

Fig. 10.3 Sum of the N and O_1 contributions

The agreement between the plots of Figs. 10.1 and 10.3 is poor but at least we have understood how the acoustic oscillations free-stream until today and are seen in the CMB TT power spectrum. There are several feature missing in Fig. 10.3: there are too many peaks, their relative height diminishes too slowly and the overall trend does not decay as in Fig. 10.1. The reason is that we have neglected baryons and diffusion damping, which we are going to tackle in the next sections.

10.3.2 Baryon Loading

The oscillations in Eq. (10.64) take place with frequency $k/\sqrt{3}$, i.e. as if the speed of sound was $1/\sqrt{3}$, i.e. the speed of sound of a pure photon fluid. We have been too radical in assuming $V_\mathrm{b} = 3\Theta_1$ in the equation for baryons. In fact we saw that this assumption is equivalent to say that $R = 0$, i.e. the baryon density is negligible with respect to the photon one. That is why photons do not feel baryons at all and baryons fluctuations oscillate in the same way as photons do.

We now take into account R up to first-order. If we consider $V_\mathrm{b}^{(0)} = 3\Theta_1$ substituted in Eq. (10.59) we get up to order R:

$$V_\mathrm{b} = 3\Theta_1 + \frac{R}{\tau'}\left(3\Theta_1' + 3\mathcal{H}\Theta_1 - k\Psi\right) \,. \tag{10.85}$$

Exercise 10.7 Combine the above equation and Eqs. (10.54)–(10.55) in order to find the following second-order equation for Θ_0:

$$\Theta_0'' + \mathcal{H}\frac{R}{1+R}\Theta_0' + \frac{k^2}{3(1+R)}\Theta_0 = -\frac{k^2\Psi}{3} - \Phi'' - \mathcal{H}\frac{R}{1+R}\Phi' \,. \tag{10.86}$$

Now the speed of sound, i.e. the quantity multiplying k^2, has been reduced:

$$c_s^2 = \frac{1}{3(1+R)} \,. \tag{10.87}$$

The extrema of the temperature fluctuation at recombination are now expected to be slightly changed, since:

$$\frac{k\eta_*}{\sqrt{3(1+R)}} = n\pi \,, \qquad (n = 1, 2, \dots) \,, \tag{10.88}$$

is now the condition defining them. Moreover, baryons are also responsible for the damping term $\mathcal{H}R\Theta_0'/(1+R)$, hence we also expect the extrema to have less and less amplitude. These features translate, once free-streamed,[2] in a relative suppression of the second peak with respect to the first one, as seen in Fig. 10.1.

This effect is due to the **baryon loading** and it is also called **baryon drag**. Physically, baryons are heavy and prevent the oscillations in Θ_0 to be symmetric, favouring compression over rarefaction. Since $R \propto a$, then we have that:

$$R' = \mathcal{H}R \,. \tag{10.89}$$

Let us write Eq. (10.86) in the following form:

$$\left(\frac{d^2}{d\eta^2} + \frac{R'}{1+R}\frac{d}{d\eta} + k^2 c_s^2\right)(\Theta_0 + \Phi) = \frac{k^2}{3}\left(\frac{\Phi}{1+R} - \Psi\right) \,. \tag{10.90}$$

The above equation cannot be solved analytically, but we can use a semi-analytic approximation, provided by Hu and Sugiyama (1996). Let us employ the WKB method and use the following ansatz:

$$(\Theta_0 + \Phi)(\eta, k) = A(\eta) e^{iB(\eta,k)} \,, \tag{10.91}$$

where $A(\eta)$ and $B(\eta, k)$ are functions to be determined via Eq. (10.90).

Exercise 10.8 Substitute this ansatz into the homogenous part of Eq. (10.90) and find the following couple of equations, by separately equating the real and imaginary parts to zero:

$$-A(B')^2 + A'' + \frac{R'}{1+R}A' + k^2 c_s^2 A = 0 \,, \tag{10.92}$$

$$2B'A' + AB'' + \frac{R'}{1+R}AB' = 0 \,. \tag{10.93}$$

---

[2] To "free-stream" means to calculate the $C_{TT,\ell}$'s weighting the solution at recombination with the spherical Bessel function of Eq. (10.24).

In the first equation, let us neglect the second and the third term with respect to the first one. That is, the oscillations provide almost at any time (except at the extrema) a much larger derivative than that of the amplitude or R. Then, the first equation is readily solved as:

$$\boxed{B(\eta, k) = k \int_0^\eta c_s(\eta') d\eta' \equiv k r_s(\eta)} \tag{10.94}$$

where in the last step we have defined the **sound horizon**, i.e. the conformal distance travelled by a sound wave propagating in the baryon photon fluid. When evaluated at recombination, $r_s(\eta_*) = 150$ Mpc and this scale is fundamental for BAO, making them **standard rulers**.

Exercise 10.9 Determine now $A(\eta)$. Show that the above equations, together with the found solution for $B(\eta, k)$, can be cast as:

$$\frac{A'}{A} = -\frac{1}{4} \frac{R'}{1+R} , \tag{10.95}$$

which gives:

$$A(\eta) = (1+R)^{-1/4} . \tag{10.96}$$

The general, approximate, solution of the homogeneous equation is then:

$$\boxed{(\Theta_0 + \Phi)(\eta, k) = \frac{1}{(1+R)^{1/4}} \left[C(k) \sin(k r_s) + D(k) \cos(k r_s) \right]} \tag{10.97}$$

The condition $|A'|$, $R' \ll |B'|$, which was employed in order to find the above solution, can be checked as follows:

$$\frac{R'}{4(1+R)^{5/4}}, R' \ll \frac{k}{\sqrt{3(1+R)}} , \tag{10.98}$$

which essentially amounts to say that:

$$k \gg R' , \tag{10.99}$$

i.e. the solution found is good on sufficiently small scales. Since $R' = \mathcal{H} R \sim R/\eta$, we must have that $k\eta \gg R$. Since R is pretty small, being at most $R_* \approx 0.6$ at recombination, this condition means any scale at early times, but sub-horizon scales at recombination.

Equation (10.97) gives us the general solution of the homogeneous part of Eq. (10.90). In order to find the general solution of the full equation we need to find a particular solution of Eq. (10.90). This can be obtained via Green's functions method, which we recall in Chap. 12. Let us define, in order to keep a more compact notation, the independent solutions of the homogeneous equation that we have just found in Eq. (10.97) as follows:

$$S_1(\eta, k) \equiv \frac{1}{(1+R)^{1/4}} \sin(kr_s) \ , \qquad S_2(\eta, k) \equiv \frac{1}{(1+R)^{1/4}} \cos(kr_s) \ . \quad (10.100)$$

Taking into account the non-homogeneous term, the general solution of Eq. (10.90) is:

$$(\Theta_0 + \Phi)(\eta, k) = C(k) S_1 + D(k) S_2 + \frac{k^2}{3} \int_0^\eta d\eta' \left[\frac{\Phi(\eta')}{1+R} - \Psi(\eta') \right] G(\eta, \eta') \ , \quad (10.101)$$

where $G(\eta, \eta')$ is the Green's function.

Exercise 10.10 As done in Chap. 12, cf. Eq. (12.121), determine the Green's function:

$$G(\eta, \eta') = \frac{S_1(\eta') S_2(\eta) - S_1(\eta) S_2(\eta')}{W(\eta')} \ , \quad (10.102)$$

using the homogeneous solution. Show that:

$$G(\eta, \eta') = \frac{1}{\sqrt{1+R}} \frac{\sin[kr_s(\eta') - kr_s(\eta)]}{W(\eta')} \ , \quad (10.103)$$

and

$$W(\eta') = -\frac{1}{\sqrt{3}(1+R)} \ . \quad (10.104)$$

We are omitting the k-dependence for simplicity.

With the above results we can write:

$$(\Theta_0 + \Phi)(\eta, k) = C(k) S_1 + D(k) S_2$$
$$+ \frac{k}{\sqrt{3}} \int_0^\eta d\eta' \left[\frac{\Phi(\eta')}{1+R(\eta')} - \Psi(\eta') \right] \sqrt{1+R(\eta')} \sin[kr_s(\eta) - kr_s(\eta')] \ . \quad (10.105)$$

For the primordial modes, in the limit $k\eta \to 0$, one gets at the dominant order:

$$(\Theta_0 + \Phi)(0, k) = D(k) \ . \quad (10.106)$$

Hence, it is the adiabatic mode which multiplies the cosine. Since sine and cosine have a $\pi/2$ phase difference, the effect of different initial conditions is to change the scales for which the effective temperature fluctuations is maximum or minimum and hence the positions of the peaks in the $C_{TT,\ell}$'s.

In the adiabatic case, we have:

$$\boxed{(\Theta_0+\Phi)(\eta,k)=(\Theta_0+\Phi)(0,k)\frac{\cos[kr_s(\eta)]}{(1+R)^{1/4}}}$$
$$\boxed{+\frac{k}{\sqrt{3}}\int_0^\eta d\eta'\left[\frac{\Phi(\eta')}{1+R}-\Psi(\eta')\right]\sqrt{1+R}\sin[kr_s(\eta)-kr_s(\eta')]} \tag{10.107}$$

This is the semi-analytic (semi because the integral has to be performed numerically) formula of Hu and Sugiyama (1996).

The above solution (10.107) can also be used for baryons. Indeed, combining Eq. (10.56) with Eq. (10.85) and then with Eq. (10.54) we get:

$$\delta_{\rm b}'=3\Theta_0'+\frac{3R}{\tau'}\left[\Theta_0''+\Phi''+\mathcal{H}(\Theta_0'+\Phi')+\frac{k^2\Psi}{3}\right]. \tag{10.108}$$

Eliminating the second derivative by means of the differential equation (10.90), we have:

$$\delta_{\rm b}'=3\Theta_0'+\frac{R}{\tau'(1+R)}\left[-k^2\Theta_0+3\mathcal{H}(\Theta_0'+\Phi')\right]. \tag{10.109}$$

Just to make a rough estimative, let us neglect the second contribution (which is divided by τ' anyway which is much larger than $\mathcal{H}$ and also than k, for suitable scales) and use the homogeneous part of Eq. (10.107). It is straightforward then to integrate $\delta_{\rm b}'$ and obtain at recombination:

$$\delta_{\rm b}(\eta_*,k)\propto\cos[kr_s(\eta_*)]=\cos\left[2\pi\frac{r_s(\eta_*)}{\lambda}\right]. \tag{10.110}$$

So the scale $r_s(\eta_*)\approx 150$ Mpc is relevant for baryons, too. Indeed, at about this scale the matter power spectrum display the BAO feature, as we saw in Chap. 9.

10.4 Diffusion Damping

In order to understand what happens to the $C_{TT,\ell}$'s when ℓ grows larger and larger we need to take into account smaller and smaller scales, because of the relation $\ell\approx k\eta_0$. As discussed earlier, for larger and larger k the ratio $-\tau'/k$ becomes smaller and smaller and so the TC approximation must be relaxed.

In this section then we investigate what happens to the temperature fluctuations when the quadrupole moment Θ_2 is taken into account. Since this analysis accounts for the behavior of very small scales which entered the horizon deep into the radiation-dominated epoch, we can neglect the gravitational potentials since these, as we saw in Chap. 9, rapidly decay.

Moreover, being deep into the radiation-dominated epoch, we can also neglect R and thus take $3\Theta_1 = V_\mathrm{b}$. Neglecting also polarisation, we have the following set of three equations for Θ_0, Θ_1 and Θ_2:

$$\Theta_0' + k\Theta_1 = 0 \,, \tag{10.111}$$

$$3\Theta_1' + 2k\Theta_2 - k\Theta_0 = 0 \,, \tag{10.112}$$

$$10\Theta_2' - 4k\Theta_1 = 9\tau'\Theta_2 \,. \tag{10.113}$$

In the last equation we can neglect Θ_2' with respect $\tau'\Theta_2$, as we already did earlier, and then find:

$$\Theta_2 = -\frac{4k}{9\tau'}\Theta_1 \,. \tag{10.114}$$

The minus sign might ring some alarm, but recall that τ' is always negative by definition.

Exercise 10.11 Combine the above condition with the remaining equations in order to find a closed equation for Θ_0:

$$\boxed{\Theta_0'' + \left(-\frac{8k^2}{27\tau'}\right)\Theta_0' + \frac{k^2}{3}\Theta_0 = 0} \tag{10.115}$$

This is the equation for an harmonic oscillator that we have already found earlier in Eq. (10.64), only that now there appears a damping term which is relevant on small scales, i.e. when $k \sim -\tau'$. Baryons also provide a damping term, cf. Eq. (10.86), but they are irrelevant in the present case since we set $R = 0$.

This damping term here depends on Θ_2 and is time-dependent. Let us consider it constant and assume a solution of the type $\Theta_0 \propto \exp(i\omega\eta)$. Substituting this ansatz in the equation, we find:

$$-\omega^2 + \left(-\frac{8k^2}{27\tau'}\right) i\omega + \frac{k^2}{3} = 0 \,. \tag{10.116}$$

The frequency must have an imaginary part, which accounts for the damping, thus let us stipulate:

$$\omega = \omega_R + i\omega_I \,, \tag{10.117}$$

Exercise 10.12 Substitute this ansatz in the equation and find:

$$\omega_R = \frac{k}{\sqrt{3}} , \qquad \omega_I = -\frac{4k^2}{27\tau'} . \tag{10.118}$$

Hence, we can write the general solution for Θ_0 as:

$$\Theta_0 \propto e^{ik\eta/\sqrt{3}} e^{-k^2/k_{\rm Silk}^2} , \tag{10.119}$$

where we have introduced the comoving diffusion length, the **Silk length**, as

$$\lambda_{\rm Silk}^2 = \frac{1}{k_{\rm Silk}^2} \equiv -\frac{4\eta}{27\tau'} . \tag{10.120}$$

What does the diffusion length physically represent? It is the comoving distance travelled by a photon in a time η, but taking into account the collisions which it is suffering, i.e. its diffusion. Let us see this in some more detail.

Since $-\tau'$ is the scattering rate, i.e. how many collisions take place per unit conformal time, then $-1/\tau'$ is the average conformal time between 2 consecutive collisions, which for a photon is also the average comoving distance between two collision, i.e. the mean free path.

Now, we have:

$$\lambda_{\rm Silk}^2 \propto -\frac{\eta}{\tau'} \propto \lambda_{\rm MFP}\eta , \tag{10.121}$$

where we have used the comoving mean free path, $\lambda_{\rm MFP}$. Now, multiply and divide by $\lambda_{\rm MFP}$ and take the square root:

$$\lambda_{\rm Silk} \propto \lambda_{\rm MFP}\sqrt{\frac{\eta}{\lambda_{\rm MFP}}} , \tag{10.122}$$

Under the square root we have the comoving distance η divided by the photon comoving mean free path. This gives us the average number of collision N which the photons experience up to the time η and hence:

$$\lambda_{\rm Silk} \propto \sqrt{N}\lambda_{\rm MFP} , \tag{10.123}$$

which is the typical relation for diffusion. Below this scales $\lambda_{\rm Silk}$ all fluctuations are suppressed because photons cannot agglomerate since they escape away. This effect is known as **Silk damping** (Silk 1967). Therefore, the behaviour of the C_l's for large l's, as seen in Fig. 10.1, is also decaying, though not exactly as in the above solution since this has to be free-streamed first.

We can do a more detailed calculation of the damping scale as follows. Let us neglect the gravitational potential and the $\ell \geq 3$ multipoles as before, but let us deal with more care of baryons and take into account polarisation. From Eq. (10.59) we have:

$$V_\mathrm{b} = 3\Theta_1 + \frac{R}{\tau'}\left(V_\mathrm{b}' + \mathcal{H}V_\mathrm{b}\right) , \tag{10.124}$$

and the six equations for the monopole, dipole and quadrupole of the temperature fluctuations and polarisation:

$$\Theta_0' + k\Theta_1 = 0 , \tag{10.125}$$
$$3\Theta_1' + 2k\Theta_2 - k\Theta_0 = \tau'(3\Theta_1 - V_\mathrm{b}) , \tag{10.126}$$
$$10\Theta_2' - 4k\Theta_1 = 9\tau'\Theta_2 - \tau'\Theta_{P0} - \tau'\Theta_{P2} , \tag{10.127}$$
$$2\Theta_{P0}' + 2k\Theta_{P1} = \tau'\Theta_{P0} - \tau'\Theta_{P2} - \tau'\Theta_2 , \tag{10.128}$$
$$3\Theta_{P1}' + 2k\Theta_{P2} - k\Theta_{P0} = 3\tau'\Theta_{P1} , \tag{10.129}$$
$$10\Theta_{P2}' - 4k\Theta_{P1} = 9\tau'\Theta_{P2} - \tau'\Theta_{P0} - \tau'\Theta_2 . \tag{10.130}$$

Now, assuming a solution of the type $\exp(i\int \omega d\eta)$ for all the above 7 variables and also assuming that $\omega \gg \mathcal{H}$, we have:

$$V_\mathrm{b} = \frac{3\Theta_1}{1 + Ri\omega\eta_c} , \tag{10.131}$$

where we have defined $\eta_c \equiv -1/\tau'$ as the the average conformal time between 2 consecutive collisions. We have thus a closed system for Θ_0, Θ_1, Θ_2, Θ_{P0}, Θ_{P1} and Θ_{P2}:

$$i\omega\Theta_0 + k\Theta_1 = 0 , \tag{10.132}$$
$$-k\Theta_0 + 3i\omega\Theta_1\left(1 + \frac{R}{1 + Ri\omega\eta_c}\right) + 2k\Theta_2 = 0 , \tag{10.133}$$
$$-4k\eta_c\Theta_1 + (10i\omega\eta_c + 9)\Theta_2 - \Theta_{P0} - \Theta_{P2} = 0 , \tag{10.134}$$
$$-\Theta_2 + (2i\omega\eta_c + 1)\Theta_{P0} + 2k\eta_c\Theta_{P1} - \Theta_{P2} = 0 , \tag{10.135}$$
$$-k\Theta_{P0} + 3(i\omega\eta_c + 1)\Theta_{P1} + 2k\eta_c\Theta_{P2} = 0 , \tag{10.136}$$
$$-\Theta_2 - \Theta_{P0} - 4k\eta_c\Theta_{P1} + (10i\omega\eta_c + 9)\Theta_{P2} = 0 . \tag{10.137}$$

We have already arranged the variables in order for the system matrix to appear clearly. The determinant of this matrix, in order to have a non trivial solution, must be zero. Considering the limit $\omega\eta_c \ll 1$, and keeping the first-order only in $\omega\eta_c$ we get:

$$\frac{k^2}{3} - \omega^2(1 + R) + \frac{2i}{30}\omega\eta_c\left[37k^2 - 285(1 + R)\omega^2 + 15\omega^2R^2\right] = 0 . \tag{10.138}$$

In order to solve for ω, let us again employ the smallness of $\omega\eta_c$ and stipulate that:

$$\omega = \omega_0 + \delta\omega \ , \tag{10.139}$$

where $\delta\omega$ is a small correction. From the above equation is then straightforward to obtain:

$$\frac{k^2}{3} - \omega_0^2(1+R) = 0 \ , \tag{10.140}$$

$$-2\omega_0\delta\omega(1+R) + \frac{2i}{30}\omega_0\eta_c\left[37k^2 - 285(1+R)\omega_0^2 + 15\omega_0^2R^2\right] = 0 \ . \tag{10.141}$$

The first equation gives the result that we have already encountered:

$$\boxed{\omega_0^2 = \frac{k^2}{3(1+R)} = k^2c_s^2} \tag{10.142}$$

which, substituted in the second equation, gives us:

$$\boxed{\delta\omega = \frac{i\eta_c k^2}{6(1+R)}\left[\frac{16}{15} + \frac{R^2}{1+R}\right]} \tag{10.143}$$

This result was obtained for the first time by Kaiser (1983). See also the derivation of Weinberg (2008).

Therefore, the evolution of the multipoles is proportional to the following factor:

$$\exp\left(i\int \omega d\eta\right) = e^{ikr_s(\eta)}e^{-k^2/k_{\rm Silk}^2} \ , \tag{10.144}$$

where

$$\boxed{\frac{1}{k_{\rm Silk}^2} \equiv -\int_0^\eta d\eta' \frac{1}{6\tau'(1+R)}\left(\frac{16}{15} + \frac{R^2}{1+R}\right)} \tag{10.145}$$

From the best fit values of the parameter of the ΛCDM model we have:

$$\boxed{d_{\rm Silk} = 0.0066 \ {\rm Mpc}} \tag{10.146}$$

10.5 Line-of-Sight Integration

The approximate solutions found earlier are based on the TC limit, which allows us to take into account just the monopole and the dipole until recombination and then to better understand the physics behind the CMB anisotropies. On the other hand, observation demands more precise calculations to be compared with and therefore, at the end, numerical computation and codes such as CLASS are needed. Even so, there is a more efficient way of computing predictions on the CMB anisotropies than dealing directly with the hierarchy of Boltzmann equation and that is to formally integrate along the photon past light-cone according to a semi-analytic technique called **line-of-sight integration**, due to Seljak and Zaldarriaga (1996), and which was the basis for the CMBFAST code.[3]

Recall the photon Boltzmann equations (5.114) and (5.115):

$$\Theta' + ik\mu\Theta = -\Phi' - ik\mu\Psi - \tau'\left[\Theta_0 - \Theta - i\mu V_{\rm b} - \frac{1}{2}\mathcal{P}_2(\mu)\Pi\right] , \tag{10.147}$$

$$\Theta'_P + ik\mu\Theta_P = -\tau'\left[-\Theta_P + \frac{1}{2}[1 - \mathcal{P}_2(\mu)]\Pi\right] , \tag{10.148}$$

where $\Pi = \Theta_2 + \Theta_{P2} + \Theta_{P0}$. Let us rewrite them as follows:

$$\Theta' + (ik\mu - \tau')\Theta = -\Phi' - ik\mu\Psi - \tau'\left[\Theta_0 - i\mu V_{\rm b} - \frac{1}{2}\mathcal{P}_2(\mu)\Pi\right] \equiv \mathcal{S}(\eta, k, \mu) , \tag{10.149}$$

$$\Theta'_P + (ik\mu - \tau')\Theta_P = -\frac{\tau'}{2}[1 - \mathcal{P}_2(\mu)]\Pi \equiv \mathcal{S}_P(\eta, k, \mu) , \tag{10.150}$$

where we have introduced two source functions on the right hand sides. Note that the dependence in on k and not on $\mathbf{k} = k\hat{z}$ because we are considering the equations for the transfer functions. Afterwards, before performing the anti-Fourier transform, we must rotate back $\hat{k}$ in a generic direction.

Let us write the left hand sides as follows:

$$\Theta' + (ik\mu - \tau')\Theta = e^{-ik\mu\eta + \tau}\frac{d}{d\eta}\left(\Theta\, e^{ik\mu\eta - \tau}\right) , \tag{10.151}$$

with a similar expression for Θ_P. Substituting these into the Boltzmann equations and integrating formally from a certain initial $\eta_i \to 0$ to today η_0, we get:

[3] https://lambda.gsfc.nasa.gov/toolbox/tb_cmbfast_ov.cfm.

$$\Theta(\eta_0)e^{-\tau(\eta_0)} = \Theta(\eta_i)e^{ik\mu(\eta_i-\eta_0)-\tau(\eta_i)} + \int_{\eta_i}^{\eta_0} d\eta\, e^{ik\mu(\eta-\eta_0)-\tau(\eta)}\mathcal{S}(\eta,k,\mu)\ , \tag{10.152}$$

$$\Theta_P(\eta_0)e^{-\tau(\eta_0)} = \Theta_P(\eta_i)e^{ik\mu(\eta_i-\eta_0)-\tau(\eta_i)} + \int_{\eta_i}^{\eta_0} d\eta\, e^{ik\mu(\eta-\eta_0)-\tau(\eta)}\mathcal{S}_P(\eta,k,\mu)\ , \tag{10.153}$$

Now recall the definition of the optical depth:

$$\tau \equiv \int_{\eta}^{\eta_0} d\eta'\, n_e\sigma_T a\ . \tag{10.154}$$

It is clear then that $\tau(\eta_0) = 0$ and, since $\eta_i \to 0$ is deep into the radiation-dominated epoch, then $\tau \propto 1/\eta$ is very large and we can neglect $\exp[-\tau(\eta_i)]$. Therefore, we are left with

$$\Theta(\eta_0,k,\mu) = \int_0^{\eta_0} d\eta\, e^{ik\mu(\eta-\eta_0)-\tau(\eta)}\mathcal{S}(\eta,k,\mu)\ , \tag{10.155}$$

$$\Theta_P(\eta_0,k,\mu) = \int_0^{\eta_0} d\eta\, e^{ik\mu(\eta-\eta_0)-\tau(\eta)}\mathcal{S}_P(\eta,k,\mu)\ . \tag{10.156}$$

where we have already implemented the limit $\eta_i \to 0$. Now we calculate the Θ_ℓ's inverting the Legendre expansion as done in Eq. (5.113) and obtain:

$$\Theta_\ell(\eta_0,k) = \frac{1}{(-i)^\ell}\int_{-1}^{1}\frac{d\mu}{2}\,\mathcal{P}_\ell(\mu)\int_0^{\eta_0} d\eta\, e^{ik\mu(\eta-\eta_0)-\tau(\eta)}\mathcal{S}(k,\eta,\mu)\ , \tag{10.157}$$

$$\Theta_{P\ell}(\eta_0,k) = \frac{1}{(-i)^\ell}\int_{-1}^{1}\frac{d\mu}{2}\,\mathcal{P}_\ell(\mu)\int_0^{\eta_0} d\eta\, e^{ik\mu(\eta-\eta_0)-\tau(\eta)}\mathcal{S}_P(k,\eta,\mu)\ , \tag{10.158}$$

The source terms have μ-dependent contributions (up to μ^2) that we can handle integrating by parts. Take for example the $-ik\mu\Psi$ contribution of $\mathcal{S}(k,\eta,\mu)$. Let I_Ψ be its integral, which can be rewritten as follows:

$$I_\Psi \equiv -\int_0^{\eta_0} d\eta\, ik\mu\Psi e^{ik\mu(\eta-\eta_0)-\tau(\eta)} = -\int_0^{\eta_0} d\eta\, \Psi e^{-\tau(\eta)}\frac{d}{d\eta}\left[e^{ik\mu(\eta-\eta_0)}\right]\ , \tag{10.159}$$

and now it is easy to integrate by parts and obtain:

$$I_\Psi = -\Psi e^{-\tau(\eta)}e^{ik\mu(\eta-\eta_0)}\Big|_0^{\eta_0} + \int_0^{\eta_0} d\eta\, e^{ik\mu(\eta-\eta_0)}\frac{d}{d\eta}\left[\Psi e^{-\tau(\eta)}\right]\ . \tag{10.160}$$

The first contribution gives $-\Psi(\eta_0)$, i.e. the gravitational potential evaluated at present time. This is just an undetectable offset that we incorporate into the definition of $\Theta_\ell(\eta_0, k)$, as the observed anisotropy, like we did at the beginning of this chapter when dealing with the free-streaming solution.

Exercise 10.13 Take care of the term containing μ^2, in $\mathcal{P}_2(\mu)$. Show that:

$$\int_0^{\eta_0} d\eta\, \tau' \mu^2 \Pi e^{ik\mu(\eta-\eta_0)-\tau(\eta)} = -\frac{1}{k^2}\int_0^{\eta_0} d\eta\, e^{ik\mu(\eta-\eta_0)} \frac{d^2}{d\eta^2}\left[\tau' \Pi e^{-\tau(\eta)}\right] . \tag{10.161}$$

Combining all the terms treated with integration by parts, we get:

$$\Theta_\ell(k,\eta_0) = \frac{1}{(-i)^\ell}\int_{-1}^{1}\frac{d\mu}{2}\,\mathcal{P}_\ell(\mu)\int_0^{\eta_0} d\eta\, e^{ik\mu(\eta-\eta_0)} \left[-\left(\Phi' + \tau'\Theta_0 + \frac{\tau'\Pi}{4}\right)e^{-\tau} + \left(\Psi e^{-\tau} - \frac{\tau' V_\mathrm{b} e^{-\tau}}{k}\right)' - \frac{3}{4k^2}\left(\tau'\Pi e^{-\tau}\right)''\right] , \tag{10.162}$$

$$\Theta_{P\ell}(k,\eta_0) = -\frac{3}{4(-i)^\ell}\int_{-1}^{1}\frac{d\mu}{2}\,\mathcal{P}_\ell(\mu)\int_0^{\eta_0} d\eta\, e^{ik\mu(\eta-\eta_0)}\left[\tau'\Pi e^{-\tau} + \frac{1}{k^2}\left(\tau'\Pi e^{-\tau}\right)''\right] . \tag{10.163}$$

Using now the relation of Eq. (10.15), we can cast the above equations as:

$$\Theta_\ell(\eta_0,k) = \int_0^{\eta_0} d\eta\, S(\eta,k)\, j_\ell\left[k(\eta_0-\eta)\right] , \tag{10.164}$$

$$\Theta_{P\ell}(\eta_0,k) = \int_0^{\eta_0} d\eta\, S_P(\eta,k)\, j_\ell\left[k(\eta_0-\eta)\right] . \tag{10.165}$$

with

$$S(\eta,k) \equiv (\Psi' - \Phi')e^{-\tau} + g\left(\Theta_0 + \frac{\Pi}{4} + \Psi\right) + \frac{1}{k}(gV_\mathrm{b})' + \frac{3}{4k^2}(g\Pi)'' , \tag{10.166}$$

$$S_P(\eta,k) \equiv \frac{3}{4}g\Pi + \frac{3}{4k^2}(g\Pi)'' , \tag{10.167}$$

where we have introduced the **visibility function**:

$$\boxed{g(\eta) \equiv -\tau' e^{-\tau}} \tag{10.168}$$

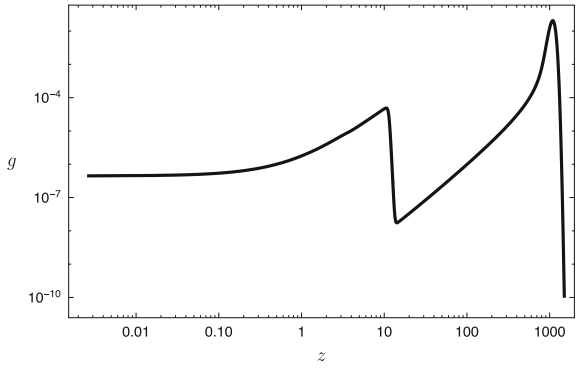

Fig. 10.4 Visibility function g as function of the redshift from the numerical calculation performed with CLASS for the standard model

Exercise 10.14 Show that the visibility function is normalised to unity, i.e.

$$\int_0^{\eta_0} d\eta \; g(\eta) = 1 \; . \tag{10.169}$$

The visibility function represents the Poissonian probability that a photon is last scattered at a time η. It is very peaked at a time that we define as the one of recombination, i.e. at $\eta = \eta_*$, because for $\eta > \eta_*$ it is basically zero, since $\tau' = 0$. Before recombination, in the radiation-dominated epoch, we saw that $-\tau' \propto 1/\eta^2$ and thus $\tau \propto 1/\eta$ and $g \propto \exp(-1/\eta)/\eta^2$, i.e. it goes to zero exponentially fast.

In Fig. 10.4 we plot the numerical calculation of the visibility function performed with CLASS for the standard model. Note the peak at about $z = 1000$, which has always been our reference for the recombination redshift. Note also another peak at about $z = 10$, representing the epoch of **reionisation**. Until now we have used the peakedness of the visibility function as if it were a Dirac delta $\delta(\eta - \eta_*)$, i.e. we have made the **sudden recombination approximation**. From Fig. 10.4 we can appreciate that it is a good approximation (mind the logarithmic scale there). As usual, in cosmology but not only, the calculations get more and more complicated and impossible to do analytically the more precision we demand.

Inserting the source terms (10.166) and (10.167) in the expressions for $\Theta_\ell(\eta_0, k)$ and $\Theta_{P\ell}(\eta_0, k)$ in the expression of Θ_ℓ and integrating by parts, we get:

$$\begin{aligned}\Theta_\ell(k, \eta_0) = &\int_0^{\eta_0} d\eta \; g \left(\Theta_0 + \Psi + \frac{\Pi}{4}\right) j_\ell \left[k(\eta_0 - \eta)\right] \\ &- \int_0^{\eta_0} d\eta \frac{g V_\mathrm{b}}{k} \frac{d}{d\eta} j_\ell \left[k(\eta_0 - \eta)\right] + \int_0^{\eta_0} d\eta \frac{3g\Pi}{4k^2} \frac{d^2}{d\eta^2} j_\ell \left[k(\eta_0 - \eta)\right] \\ &+ \int_0^{\eta_0} d\eta \; e^{-\tau} (\Psi' - \Phi') j_\ell \left[k(\eta_0 - \eta)\right] \; ,\end{aligned} \tag{10.170}$$

$$\Theta_{P\ell}(k,\eta_0) = \int_0^{\eta_0} d\eta\ \frac{3g\Pi}{4} j_\ell\left[k(\eta_0-\eta)\right] + \int_0^{\eta_0} d\eta \frac{3g\Pi}{4k^2}\frac{d^2}{d\eta^2} j_\ell\left[k(\eta_0-\eta)\right]\ . \tag{10.171}$$

Assuming the visibility function to be a Dirac delta $\delta(\eta-\eta_*)$, i.e. the sudden recombination mentioned earlier, and neglecting Π, we recover formula (10.24). Note that neglecting Π no polarisation is present. Indeed, from the above equation we see that a non-zero quadrupole moment of the photon distribution at recombination is essential in order to have polarisation.

The above equations still need the Boltzmann hierarchy in order to be integrated, but just up to $\ell = 4$ (because Θ_2 and Θ_4 moments are contained in the equation for Θ_3') and hence are much more convenient from the computational point of view.

The partial wave expansion of Θ given in Eq. (7.77):

$$\Theta(k,\mu) = \sum_\ell (-i)^\ell (2\ell+1)\mathcal{P}_\ell(\mu)\Theta_\ell(k)\ , \tag{10.172}$$

and that we have used in the above calculations is valid as long as $\hat{k} = \hat{z}$. Now we have to rotate it in a general direction before performing the Fourier anti-transform. The task is simple because the temperature fluctuation is a scalar. Therefore:

$$\Theta(k,\hat{k}\cdot\hat{p}) = \sum_\ell (-i)^\ell (2\ell+1)\mathcal{P}_\ell(\hat{k}\cdot\hat{p})\Theta_\ell(k)\ . \tag{10.173}$$

The same is not true for Θ_P, since the Stokes parameters are not scalars.

Using the definition of $a_{T,\ell m}$ given in Eq. (7.73) we can then write:

$$a^S_{T,\ell m} = \int d^2\hat{n}\ Y_\ell^{m*}(\hat{n}) \sum_l (-i)^\ell (2\ell+1) \int \frac{d^3\mathbf{k}}{(2\pi)^3}\mathcal{P}_\ell(\hat{k}\cdot\hat{p})\alpha(\mathbf{k})\Theta_\ell(k)\ . \tag{10.174}$$

The integration is over $d^2\hat{n}$, hence we must change $\hat{p}\to\hat{n} = -\hat{p}$ in the Legendre polynomial. This gives an extra $(-1)^\ell$ factor, due to the parity of the Legendre polynomials, and then using the addition theorem we obtain:

$$a^S_{T,\ell m} = \int d^2\hat{n}\ Y_\ell^{m*}(\hat{n}) \sum_l i^\ell (2\ell+1) \int \frac{d^3\mathbf{k}}{(2\pi)^3}\alpha(\mathbf{k})\frac{4\pi}{2\ell'+1} \sum_{m'=-\ell'}^{\ell'} Y_{\ell'}^{*m'}(\hat{k}) Y_{\ell'}^{m'}(\hat{n})\Theta_\ell(k)\ . \tag{10.175}$$

Now the integration over the whole solid angle can be performed and the orthonormality of the spherical harmonics can be employed, obtaining thus:

$$\boxed{a^S_{T,\ell m} = 4\pi i^\ell \int \frac{d^3\mathbf{k}}{(2\pi)^3} Y^{m*}_\ell(\hat{k})\alpha(\mathbf{k})\Theta_\ell(k)} \tag{10.176}$$

This formula, together with Eq. (10.170) allows us to explicitly calculate the scalar contribution to the $a_{T,\ell m}$'s. Earlier, we have focused on the $C_{TT,\ell}$'s only, for which the calculations are simpler because there is no need of performing a spatial rotation, but we need to know the explicit form of the $a_{T,\ell m}$'s in order to compute the TE correlation spectrum of Eq. (7.87).

10.6 Finite Thickness Effect and Reionization

In this section we discuss two more effects that influence the CMB spectrum, namely the finite thickness effect and the reionisation. The first one is related to the fact that the visibility function g in Fig. 10.4 is very peaked but it is not a Dirac delta. In other words, CMB photons do not last scatter all at once at η_* but during a finite amount of time say $\Delta\eta_*$. This is the **finite thickness effect**. Physically, on scales smaller than the thickness $\Delta\eta_*$ we expect fluctuations to be washed out because they are averaged over a finite amount of time. This is similar to what is called **Landau damping** (although the latter arises from a spread in frequency and not in time). It may seem that Landau damping is a small effect, but actually is of the same order of Silk damping and therefore it must be taken into account.

Let us take advantage of this investigation and derive the form of the visibility function here. The question is: what is the probability that a photon last scatter during some sufficiently small interval between the instants η and $\eta + \Delta\eta$? The time interval $\Delta\eta$ is sufficiently small so that only one collision can take place into it. The attentive reader has noticed that this is the same requirement we make when we derive the Poisson distribution, cf. Chap. 12, which in fact rules the statistics of e.g. scattering process.

So, we divide the time interval $\eta_0 - \eta$ in many, i.e. $N \equiv (\eta_0 - \eta)/\Delta\eta$, intervals and write the probability as:

$$\Delta P = \frac{\Delta\eta}{\eta_c(\eta)}\left[1 - \frac{\Delta\eta}{\eta_c(\eta_1)}\right]\left[1 - \frac{\Delta\eta}{\eta_c(\eta_2)}\right]\ldots\left[1 - \frac{\Delta\eta}{\eta_c(\eta_N)}\right], \tag{10.177}$$

where recall that $\eta_c \equiv -1/\tau'$ is the average time between two consecutive collisions and it is time-dependent. We have chosen the time interval $\Delta\eta$ small enough in order for $\Delta\eta/\eta_c$ to be the probability of having one scattering during its duration and hence $1 - \Delta\eta/\eta_c$ being that of having no scattering. Now, in the limit $\Delta\eta \to 0$ we can write:

$$dP = \frac{d\eta}{\eta_c}\exp\left(-\int_\eta^{\eta_0}\frac{d\eta}{\eta_c}\right) = -\tau'\exp\left[-\tau(\eta)\right]d\eta = g(\eta)d\eta\,, \tag{10.178}$$

i.e. the visibility function defined in Eq. (10.168) appears. As we have anticipated, the maximum of the visibility function occurs in a time that we dub η_*, i.e. the recombination time if we make the assumption of sudden recombination. From the condition for the extrema of a function:

$$g'(\eta) = -\tau'' e^{-\tau} + (\tau')^2 e^{-\tau} = 0 \,, \tag{10.179}$$

we get:

$$-\tau'' = (\tau')^2 \,, \tag{10.180}$$

as the condition which defines η_*. Therefore, employing the definition of the optical depth, we get:

$$(n_e \sigma_{\rm T} a)'_* = -(n_e \sigma_{\rm T} a)^2_* \,, \tag{10.181}$$

where the derivative is evaluated at η_*, as well as the function on the right hand side. Now, let us write the free-electron number density as $n_e = X_e n_{\rm b}$, i.e. introducing the free-electron fraction and the baryon number density and recall from Boltzmann equation, cf. Chap. 3, that:

$$X'_e = -\frac{1.44 \times 10^4}{z} \mathcal{H} X_e \,. \tag{10.182}$$

Evaluating the above equation at η_* and combining it with the extrema condition for the visibility function, we get:

$$X_e(\eta_*) \approx \frac{1.44 \times 10^4}{z_* (n_{\rm b} \sigma_{\rm T} a)_*} \mathcal{H}(\eta_*) \equiv \frac{K}{(n_{\rm b} \sigma_{\rm T} a)_*} \mathcal{H}(\eta_*) \,, \tag{10.183}$$

and from this we get the recombination redshift $z_* \approx 1050$.

Let us approximate the visibility function by expanding it about its maximum:

$$g(\eta) = \exp[\ln(-\tau') - \tau] \approx \exp\left[-\frac{1}{2}[\tau - \ln(-\tau')]''_* (\eta - \eta_*)^2\right] \,, \tag{10.184}$$

i.e. we have a Gaussian function. Now we determine the second derivative, and hence the variance of the distribution by using Boltzmann equation and employing the following approximation: we consider only the first derivative of X_e to be different from zero. All the other quantities are approximately constant indeed since recombination takes place quite rapidly. So, we can write:

$$\left(\tau' - \frac{\tau''}{\tau'}\right)'_* = \left(-n_{\rm b} X_e \sigma_{\rm T} a - \frac{n_{\rm b} X'_e \sigma_{\rm T} a}{n_{\rm b} X_e \sigma_{\rm T} a}\right)'_* \,. \tag{10.185}$$

Now, within our approximation X'_e / X_e is constant, and thus:

$$\left(\tau' - \frac{\tau''}{\tau'}\right)'_* = -(n_{\rm b} X'_e \sigma_{\rm T} a)_* = (n_{\rm b} X_e \sigma_{\rm T} a)^2_* = K^2 \mathcal{H}(\eta_*)^2 \,. \tag{10.186}$$

Hence the visibility function can be approximated as a Gaussian function:

$$g(\eta) \approx \frac{K\mathcal{H}_*}{\sqrt{2\pi}} \left[-\frac{1}{2} (K\mathcal{H}_*)^2 (\eta - \eta_*)^2 \right] , \tag{10.187}$$

with variance $1/(K\mathcal{H}_*)$.

When we substitute this approximation of the visibility function in the line-of-sight integrals of Eqs. (10.170) and (10.171) we can extract the spherical Bessel functions as $j_l[k(\eta_0 - \eta_*)]$, since η_0 is much larger than any conformal time about recombination, and the other integrals are oscillating functions of $kr_s(\eta)$, as we saw in Eq. (10.107). We can approximate this about η_*, as follows:

$$kr_s(\eta) = k \int_0^\eta d\eta' \frac{1}{\sqrt{3(1+R)}} \approx kr_s(\eta_*) + \frac{k}{\sqrt{3(1+R_*)}} (\eta - \eta_*) \,. \tag{10.188}$$

Hence, we have finally a conformal time Gaussian integral of the following type:

$$\int_{-\infty}^{\infty} d\eta \exp\left[-\frac{1}{2} (K\mathcal{H}_*)^2 (\eta - \eta_*)^2 + \frac{ik}{\sqrt{3(1+R_*)}} (\eta - \eta_*) \right] . \tag{10.189}$$

Now, using the formula for the Gaussian integral:

$$\int_{-\infty}^{\infty} e^{-ax^2 + bx} dx = \sqrt{\frac{\pi}{a}} e^{b^2/4a} \,, \tag{10.190}$$

we can conclude that the Θ_ℓ's get an additional damping factor of the following form:

$$\exp\left[-\frac{k^2}{6(1+R_*)(K\mathcal{H}_*)^2} \right] , \tag{10.191}$$

so a new damping scale appears:

$$\boxed{d^2_{\rm Landau} = \frac{1}{k^2_{\rm Landau}} \equiv \frac{1}{6(1+R_*)(K\mathcal{H}_*)^2}} \tag{10.192}$$

which, following Weinberg (2008), we call **Landau damping scale**. For the ΛCDM model best fit parameters we have:

$$\boxed{d_{\rm Landau} \approx 0.0048 \text{ Mpc}} \tag{10.193}$$

Now let us turn to reionisation. At a redshift of about 10 hydrogen gets ionised again by the ultraviolet radiation of the first structures. Hence, the free-electron fraction grows again increasing the probability of a CMB photon to be scattered again, cf. the extra bump in the visibility function in Fig. 10.4. Following the calculation done above in order to obtain the visibility function, we know that the probability for a photon not to be scattered from reionisation until today is:

$$\exp[-\tau(\eta_{\rm reion})] \,, \tag{10.194}$$

and of course the one for being scattered is 1 minus the above quantity, which we compute now:

$$\tau(\eta_{\rm reion}) = \int_{\eta_{\rm reion}}^{\eta_0} d\eta \, n_e \sigma_{\rm T} a = \sigma_{\rm T} \int_0^{z_{\rm reion}} \frac{dz}{(1+z)^2 \mathcal{H}} n_e \,. \tag{10.195}$$

For the free-electron number density we can write:

$$n_e = 0.88 n_{\rm b} X_e = 0.88 \frac{3H_0^2}{8\pi m_{\rm b}} \Omega_{\rm b0} (1+z)^3 \,, \tag{10.196}$$

where the factor 0.88 is due to the fact that not all the baryons are electrons or protons, but there are also neutrons in Helium nuclei. Assuming matter-domination and instantaneous reionisation, i.e.

$$\mathcal{H}^2 = H_0^2 \Omega_{\rm m0} (1+z)^3 \,, \tag{10.197}$$

and $X_e = 1$ for $z < z_{\rm reion}$, we get:

$$\tau(z_{\rm reion}) \approx 0.04 \frac{\Omega_{\rm b0} h^2}{\sqrt{\Omega_{\rm m0} h^2}} z_{\rm reion}^{3/2} \,. \tag{10.198}$$

Hence, the probability for a CMB photon not to be scattered for reionisation taking place at redshift $z_{\rm reion} = 10$ is about 0.99, i.e. very high. Those photons which are scattered are mixed up, hence the correlation in their temperature is destroyed. So, the effect of reionisation on the $C_{TT,\ell}$'s is simply to weigh them by a factor $\exp(-2\tau_{\rm reion})$, the factor 2 appearing because the spectrum is a quadratic function of the temperature fluctuations.

10.7 Cosmological Parameters Determination

In this section we discuss how the CMB TT spectrum, i.e. the $C_{TT,\ell}$'s, are sensitive to the cosmological parameters. We have learned in this chapter about many quantities which are of relevance in forming the shape of the spectrum but we have not actually

derived an analytic, approximated formula in order to see this explicitly. These can be found in Mukhanov (2005) and Weinberg (2008). Here instead we plot with CLASS various spectra for varying parameters and discuss the physics behind the changes.

Note that, for the standard Λ model, 6 of the overall parameters are usually left free and constrained by observation:

1. The amplitude of the primordial power spectrum: A_S;
2. The primordial tilt: n_S;
3. The baryonic abundance: $\Omega_{b0}h^2$;
4. The CDM abundance: $\Omega_{c0}h^2$;
5. The reionization epoch: z_{reion};
6. The sound horizon at recombination: $r_s(\eta_*)$, which is related to the Hubble constant value H_0.

The other parameters can be derived by these ones. In particular, the amount of radiation is already well known by measuring the CMB temperature and so the amount of Λ and curvature is determined via the positions of the peaks, which depend on $r_s(\eta_*)$, which in turn depends on the baryon content.

In Figs. 10.5 and 10.6 we start to show the numerical calculation of CMB TT power spectrum decomposed in the contributions discussed in this chapter. See also Wands et al. (2016). We consider the ΛCDM as fiducial model.

In Fig. 10.7 we show what happens to CMB TT the spectrum for $\Omega_{b0}h^2 = 0.010, 0.014, 0.018, 0.022, 0.026, 0.030, 0.034$. Taking the first peak height as reference, the larger the value of $\Omega_{b0}h^2$ is, the higher the peak is. When we vary one of the density parameters, since their sum must be equal to one that means that also something else must vary. In this case we have chosen to vary Ω_Λ.

Why so? We have seen that baryons loading makes compression favoured over rarefaction and hence the first and the third peaks are higher for higher values of

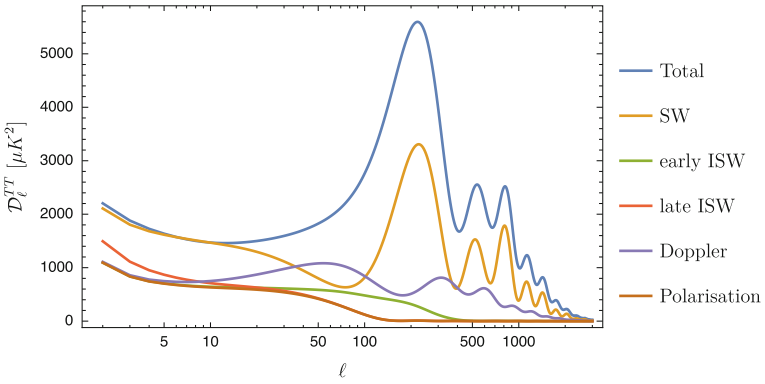

Fig. 10.5 Total CMB TT power spectrum (blue line) computed with CLASS and decomposed in the physically different contributions: Sachs-Wolfe effect (yellow line), early-times ISW effect (green line), late-times ISW effect (red line), Doppler effect (purple line), and polarisation (brown line)

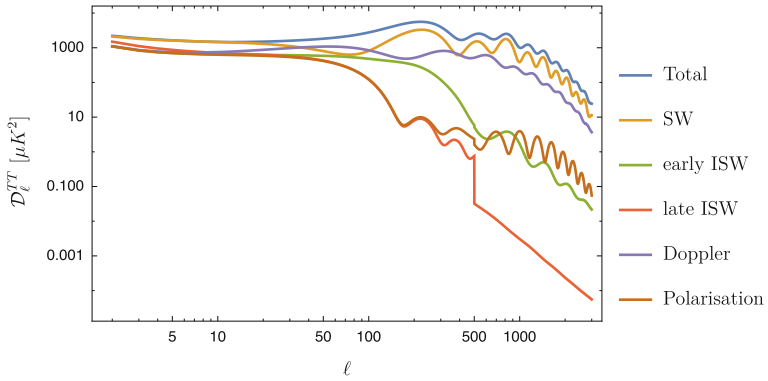

Fig. 10.6 Same as Fig. 10.5 but in logarithmic scale, in order to better distinguish the weakest contributions

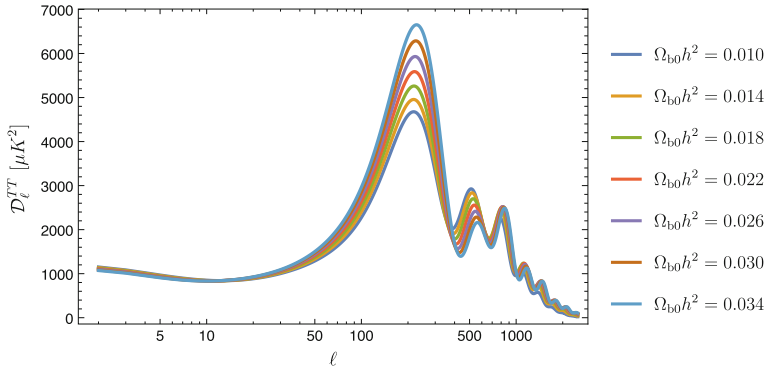

Fig. 10.7 CMB TT power spectrum computed with CLASS and varying $\Omega_{b0}h^2$. From the lowest first peak to the highest: $\Omega_{b0}h^2 = 0.010, 0.014, 0.018, 0.022, 0.026, 0.030, 0.034$

$\Omega_{b0}h^2$, but the second one is lower. In other words, the peaks relative height is very sensitive to the baryon content. The position of the first peak does not change much because it is most sensitive to the spatial curvature and this has been fixed to zero. Finally, the curves for larger $\Omega_{b0}h^2$, as we commented, have less Ω_Λ and therefore less ISW effect. For these reason they are slightly lower for small ℓ.

In Fig. 10.8 we show what happens to CMB TT the spectrum for $\Omega_{c0}h^2 = 0.09, 0.10, 0.11, 0.12, 0.13, 0.14, 0.15$. Taking the first peak height as reference, the larger the value of $\Omega_{c0}h^2$ is, the lower the peak is. This behaviour is the opposite of the one that we found by varying $\Omega_{b0}h^2$. Mostly CDM intervenes through the SW effect since it dominates the gravitational potential Ψ at recombination. The first peak is affected more because it corresponds to large scales, basically the horizon at recombination, and there the transfer function is approximately unit, meaning that $-\Psi$ is as large as possible. The subsequent peaks correspond to scales which entered the horizon much earlier and therefore the CDM influence there is weak.

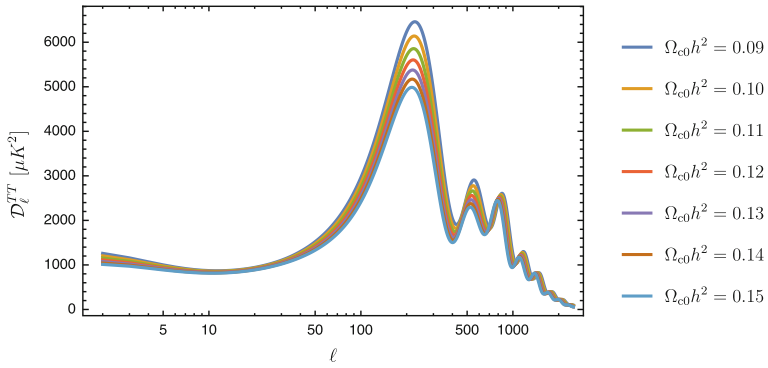

Fig. 10.8 CMB TT power spectrum computed with CLASS and varying $\Omega_{c0}h^2$. From the highest first peak to the lowest: $\Omega_{c0}h^2 = 0.09, 0.10, 0.11, 0.12, 0.13, 0.14, 0.15$

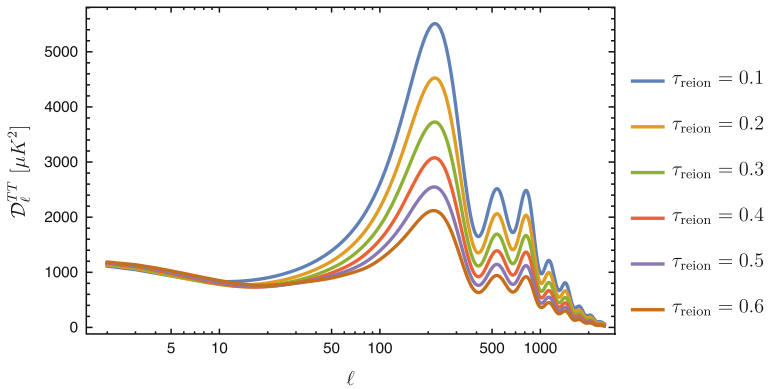

Fig. 10.9 CMB TT power spectrum computed with CLASS and varying τ_{reion}. From the highest first peak to the lowest: $\tau_{\text{reion}} = 0.1, 0.2, 0.3, 0.4, 0.5, 0.6, 0.7$

In this case also we have chosen to vary Ω_Λ in order to keep the total density budget. Indeed, the more CDM, the less Λ and the less ISW effect, as expected.

In Fig. 10.9 we show what happens to CMB TT the spectrum for $\tau_{\text{reion}} = 0.1, 0.2, 0.3, 0.4, 0.5, 0.6, 0.7$. As we have commented in the previous section, the overall effect of reionisation is simple because it happens very lately: a damping of the order $\exp(-2\tau_{\text{reion}})$ for multipoles larger than a certain ℓ_{reion} which we infer to be about 10 from the plots in Fig. 10.9.

From Fig. 10.10 we can appreciate how the CMB TT power spectrum is affected by the spatial geometry of the universe. From the leftmost spectrum to the rightmost one $\Omega_{K0} = -0.2, -0.1, 0, 0.1, 0.2$. Hence, the position of the first peak is of great importance in order to determine whether our universe is closed or open. Note that the flat case is a limiting value which we cannot determine observationally, because

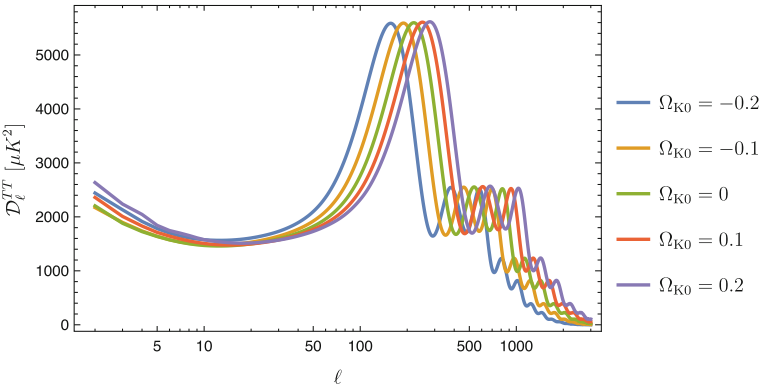

Fig. 10.10 CMB TT power spectrum computed with CLASS and varying Ω_{K0}. From the left to the right: $\Omega_{K0} = -0.2, -0.1, 0, 0.1, 0.2$

of the experimental error; we can only conclude that observation is consistent with $\Omega_{K0} = 0$, i.e. this value is not ruled out.

As we saw in Eq. (10.107), the length scale associated to the acoustic peaks is the sound horizon at recombination:

$$r_s(\eta_*) = \int_0^{\eta_*} c_s d\eta \,, \tag{10.199}$$

where the speed of sound of the baryon-photon plasma is given by Eq. (10.87):

$$c_s^2 = \frac{1}{3(1+R)} = \frac{4\Omega_{\gamma 0}}{3(4\Omega_{\gamma 0} + 3\Omega_{b0} a)} \,. \tag{10.200}$$

The physical sound horizon is given by:

$$r_s^{\rm phys}(z_*) = \int_0^{t_*} c_s(t) dt = \int_{z_*}^{\infty} dz \frac{c_s(z)}{H(z)(1+z)} \,, \tag{10.201}$$

i.e. integrating the lookback time. We need the physical quantity in order to relate it with the angular-diameter distance to recombination:

$$d_{\rm A}(z_*) = \frac{1}{(1+z_*)} \int_0^{z_*} \frac{dz}{H(z)} \,, \tag{10.202}$$

and thus estimate the multipole corresponding to the first peak:

$$\ell_{\rm 1st} \approx \frac{1}{\theta_{\rm 1st}} = \frac{d_{\rm A}(z_*)}{r_s^{\rm phys}(z_*)} \,. \tag{10.203}$$

Let us approximate the physical sound horizon by assuming c_s constant and a matter-dominated universe. We have thus:

$$r_s^{\rm phys}(z_*) \approx \frac{c_s}{H_0\sqrt{\Omega_{\rm m0}}}\int_{z_*}^{\infty}\frac{dz}{(1+z)^{5/2}} = \frac{2c_s}{3H_0\sqrt{\Omega_{\rm m0}}}\frac{1}{(1+z_*)^{3/2}}\ , \tag{10.204}$$

and for the angular-diameter distance we also assume a matter plus Λ universe:

$$d_{\rm A}(z_*) = \frac{1}{H_0(1+z_*)}\int_0^{z_*}\frac{dz}{\sqrt{\Omega_{\rm m0}(1+z)^3+(1-\Omega_{\rm m0})}}\ . \tag{10.205}$$

Exercise 10.15 Show that $d_{\rm A}(z_*)$ can be approximated as:

$$d_{\rm A}(z_*) \approx \frac{2}{7H_0(1+z_*)\sqrt{\Omega_{\rm m0}}}(9-2\Omega_{\rm m0}^3)\ . \tag{10.206}$$

Hence, we have:

$$\ell_{\rm 1st} \approx 0.74\sqrt{1+z_*}(9-2\Omega_{\rm m0}^3) \approx 220\ , \tag{10.207}$$

which clearly shows how the position of the first peak changes as function of the total matter content.

In Fig. 10.11 we show how the initial conditions dramatically affect the CMB TT power spectrum and how the adiabatic ones are favoured by observation (when comparing with the data points of Fig. 10.1).

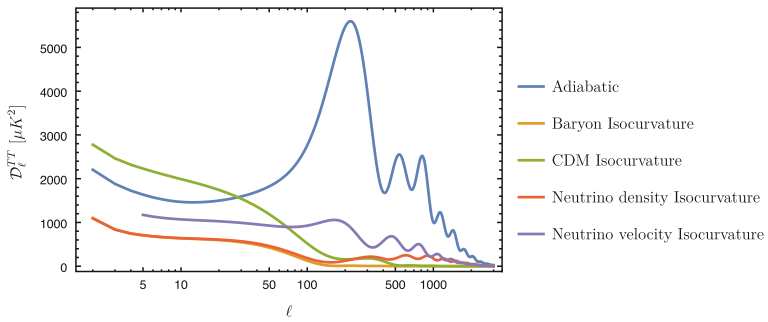

Fig. 10.11 CMB TT power spectrum computed with CLASS and varying initial conditions: adiabatic (blue line), baryon isocurvature (yellow line), CDM isocurvature (green line), neutrino density isocurvature (red line), neutrino velocity isocurvature (purple line)

10.8 Tensor Contribution to the CMB TT Correlation

Tensor perturbations also contribute to generate temperature anisotropies, as we see in Eq. (5.138), which we report here after renormalising to the primordial mode $\beta(\mathbf{k}, \lambda)$, cf. Eq. (7.101):

$$\left(\frac{\partial}{\partial\eta} + ik\mu - \tau'\right)\Theta^{(T)}(\eta, k, \mu) + \frac{h'^T}{2} = -\tau'\left[\frac{3}{70}\Theta_4^{(T)} + \frac{1}{7}\Theta_2^{(T)} + \frac{1}{10}\Theta_0^{(T)} - \frac{3}{70}\Theta_{P4}^{(T)} + \frac{6}{7}\Theta_{P2}^{(T)} - \frac{3}{5}\Theta_{P0}^{(T)}\right] \equiv -\tau'\mathcal{S}^T(\eta, k)\,, \tag{10.208}$$

$$\left(\frac{\partial}{\partial\eta} + ik\mu - \tau'\right)\Theta_P^{(T)}(\eta, k, \mu) = \tau'\mathcal{S}^T(\eta, k)\,, \tag{10.209}$$

The label λ representing the two possible states of helicity is absent because of the renormalisation with $\beta(\mathbf{k}, \lambda)$. It represents the fact that the evolution of the two helicities is the same.

The line-of-sight solutions of the above equations are the following:

$$\Theta^{(T)}(\eta_0, k, \mu) = \int_0^{\eta_0} d\eta\, e^{ik\mu(\eta-\eta_0)-\tau}\left[-h'^T/2 - \tau'\mathcal{S}^T(\eta, k)\right]\,, \tag{10.210}$$

$$\Theta_P^{(T)}(\eta_0, k, \mu) = \int_0^{\eta_0} d\eta\, e^{ik\mu(\eta-\eta_0)-\tau}\tau'\mathcal{S}^T(\eta, k)\,. \tag{10.211}$$

We now focus on $\Theta^{(T)}(\eta_0, k, \mu)$. Defining:

$$S^T(\eta, k) \equiv e^{-\tau}\left[-h'^T/2 - \tau'\mathcal{S}^T(\eta, k)\right]\,, \tag{10.212}$$

and using Eqs. (5.131) and (5.32), the tensor contribution to the temperature fluctuation is made up of the sum of the following two contributions:

$$f_\lambda(k\hat{z}, \hat{p}) \equiv 4\sqrt{\frac{\pi}{15}}Y_2^\lambda(\hat{p})\int_0^{\eta_0} d\eta\, S^T(\eta, k)e^{-i\mu kr(\eta)}\,, \tag{10.213}$$

where $r(\eta) \equiv \eta_0 - \eta$ and where we stress that the result holds true for $\hat{k} = \hat{z}$ since this was the condition under which we derived the Boltzmann equation for photons. We cannot yet sum over λ because we have to include $\beta(\mathbf{k}, \lambda)$ first. For this reason, we shall work on $f_\lambda(k\hat{z}, \hat{p})$.

In order to investigate temperature fluctuations in the sky, we need to anti-transform $\Theta^{(T)}(\mathbf{k}, \hat{p})$ in order to employ the usual expansion:

$$\Theta^{(T)}(\hat{n}) = \sum_{\ell m} a^T_{T,\ell m}Y_\ell^m(\hat{n})\,, \quad a^T_{T,\ell m} = \int d^2\hat{n}\; Y_\ell^{m*}(\hat{n})\Theta^{(T)}(\hat{n})\,. \tag{10.214}$$

So, let us proceed as follows. We trade $\hat{p}$ for the line-of-sight $\hat{n} = -\hat{p}$ and use the expansion of a plane wave in spherical harmonics:

$$e^{i\hat{k}\cdot\hat{n}kr} = \sum_{LM} i^L Y_L^{M*}(\hat{k}) Y_L^M(\hat{n}) j_L(kr) \,, \tag{10.215}$$

in Eq. (10.213).

Exercise 10.16 First of all, since $\hat{k} = \hat{z}$ then show that:

$$Y_L^{M*}(\hat{k}) = Y_L^{M*}(\hat{z}) = \delta_{M0}\sqrt{\frac{2L+1}{4\pi}} \,, \tag{10.216}$$

i.e. for $\theta = 0$ (representing the $\hat{z}$ direction) the spherical harmonics are non-vanishing only if $M = 0$.

Therefore, we can write:

$$f_\lambda(k\hat{z}, \hat{n}) = \frac{2}{\sqrt{15}} Y_2^\lambda(\hat{n}) \sum_L i^L \sqrt{2L+1} Y_L^0(\hat{n}) \int_0^{\eta_0} d\eta \; S^T(\eta, k) j_L(kr) \,. \tag{10.217}$$

The idea is now to perform a rotation in order to put $\hat{k}$ in a generic direction. But then also $\hat{n}$ rotates and therefore we need to know how a spherical harmonics behaves under rotations. In order to deal with just one spherical harmonic we take advantage of the following decomposition:

$$Y_2^{\pm 2}(\hat{n}) Y_L^0(\hat{n}) = \sqrt{\frac{5(2L+1)}{4\pi}} \sum_{L'} \sqrt{2L'+1} \begin{pmatrix} L & 2 & L' \\ 0 & \pm 2 & \mp 2 \end{pmatrix} \begin{pmatrix} L & 2 & L' \\ 0 & 0 & 0 \end{pmatrix} Y_{L'}^{\pm 2}(\hat{n}) \,, \tag{10.218}$$

where we have employed the **Wigner 3j-symbols**, which are coefficients appearing in the quantum theory of angular momentum, when we combine two angular momenta and we want to write the state of total angular momentum as a linear combination on the basis of the tensor product of the two combined angular momenta. They are an alternative to the (perhaps more commonly used) Clebsch-Gordan coefficient See e.g. Landau and Lifshits (1991) and Weinberg (2015).

This expansion allows us to deal with just one spherical harmonics. Now we take advantage of the properties of the spherical harmonics under spatial rotation, i.e.

$$\boxed{Y_\ell^m(R\hat{n}) = \sum_{m'=-\ell}^{\ell} D^{(\ell)}_{m'm}(R^{-1}) Y_\ell^{m'}(\hat{n})} \tag{10.219}$$

where the $D^{(\ell)}_{m'm}$ are the elements of the **Wigner D-matrix**. See Landau and Lifshits (1991) for more detail. The above R is a generic rotation. Of course, we are interested in a $R(\hat{k})$ rotation which brings $\hat{k}$ in a generic direction. Hence, we can write:

$$f_\lambda(\mathbf{k}, \hat{n}) = \sum_L i^L \frac{2L+1}{\sqrt{3\pi}} \sum_{L'} \sqrt{2L'+1} \begin{pmatrix} L & 2 & L' \\ 0 & \lambda & -\lambda \end{pmatrix}$$
$$\begin{pmatrix} L & 2 & L' \\ 0 & 0 & 0 \end{pmatrix} \sum_{m'} D^{(L')}_{m'\lambda}[R(\hat{k})] Y^{m'}_{L'}(\hat{n}) \int_0^{\eta_0} d\eta \; S^T(\eta, k) j_L(kr) \; . \tag{10.220}$$

Here we have dubbed $R\hat{n}$ the original line of sight and $\hat{n}$ the resulting one after the rotation.

Now we can perform the Fourier anti-transform. Let us multiply $f_\lambda(\mathbf{k}, \hat{n})$ by $\beta(\mathbf{k}, \lambda)$ and $Y_\ell^{m*}(\hat{n})$ and integrate over $d^2\hat{n}$ in order to obtain the $a^T_{T,\ell m}$'s. We obtain:

$$a^T_{\ell m,\pm 2} = \sum_L i^L \frac{2L+1}{\sqrt{3\pi}} \sqrt{2\ell+1} \begin{pmatrix} L & 2 & \ell \\ 0 & \pm 2 & \mp 2 \end{pmatrix}$$
$$\begin{pmatrix} L & 2 & \ell \\ 0 & 0 & 0 \end{pmatrix} \int \frac{d^3\mathbf{k}}{(2\pi)^3} D^{(\ell)}_{m\pm 2}[R(\hat{k})] \beta(\mathbf{k}, \pm 2) \int_0^{\eta_0} d\eta \; S^T(\eta, k) j_L(kr) \; . \tag{10.221}$$

We have used here the orthonormality relation of the spherical harmonics and distinguished the contributions from different helicities. Of course $a_{\ell m} = a_{\ell m,+2} + a_{\ell m,-2}$.

It is now time to compute the $3j$ symbols and to perform the summation over L. A general formula for those was obtained in Racah (1942), but we can read their expression from Landau and Lifshits (1991). We then have the only following non-vanishing occurrences:

$$\begin{pmatrix} \ell & 2 & \ell \\ 0 & 0 & 0 \end{pmatrix} = (-1)^{\ell+1} \sqrt{\frac{\ell(\ell+1)}{(2\ell-1)(2\ell+1)(2\ell+3)}} \; , \tag{10.222}$$

$$\begin{pmatrix} \ell+2 & 2 & \ell \\ 0 & 0 & 0 \end{pmatrix} = (-1)^{\ell} \sqrt{\frac{3(\ell+1)(\ell+2)}{2(2\ell+1)(2\ell+3)(2\ell+5)}} \; , \tag{10.223}$$

$$\begin{pmatrix} \ell-2 & 2 & \ell \\ 0 & 0 & 0 \end{pmatrix} = (-1)^{\ell} \sqrt{\frac{3\ell(\ell-1)}{2(2\ell-3)(2\ell-1)(2\ell+1)}} \; . \tag{10.224}$$

In particular, there is no contribution coming from $L = \ell \pm 1$. The other three relevant (i.e. not considering those for $L = \ell \pm 1$ which are non-vanishing in this case) symbols are:

$$\begin{pmatrix} \ell & 2 & \ell \\ 0 & \pm 2 & \mp 2 \end{pmatrix} = (-1)^{\ell} \sqrt{\frac{3(\ell-1)(\ell+2)}{2(2\ell-1)(2\ell+1)(2\ell+3)}} , \tag{10.225}$$

$$\begin{pmatrix} \ell+2 & 2 & \ell \\ 0 & \pm 2 & \mp 2 \end{pmatrix} = (-1)^{\ell} \frac{1}{2} \sqrt{\frac{(\ell-1)\ell}{(2\ell+1)(2\ell+3)(2\ell+5)}} , \tag{10.226}$$

$$\begin{pmatrix} \ell-2 & 2 & \ell \\ 0 & \pm 2 & \mp 2 \end{pmatrix} = (-1)^{\ell} \frac{1}{2} \sqrt{\frac{(\ell+1)(\ell+2)}{(2\ell-3)(2\ell-1)(2\ell+1)}} , \tag{10.227}$$

Exercise 10.17 Derive the above expressions for the relevant Wigner $3j$ symbols given in Landau and Lifshits (1991) and put them in Eq. (10.221). Show that:

$$a^T_{T,\ell m,\pm 2} = -i^{\ell} \sqrt{\frac{(2\ell+1)(\ell+2)!}{8\pi(\ell-2)!}} \int \frac{d^3\mathbf{k}}{(2\pi)^3} D^{(\ell)}_{m\pm 2}[R(\hat{k})]\beta(\mathbf{k}, \pm 2) \int_0^{\eta_0} d\eta \; S^T(\eta, k) \left[\frac{j_{\ell-2}(kr)}{(2\ell-1)(2\ell+1)} + \frac{2j_{\ell}(kr)}{(2\ell-1)(2\ell+3)} + \frac{j_{\ell+2}(kr)}{(2\ell+1)(2\ell+3)} \right] . \tag{10.228}$$

Recall that $r = r(\eta) \equiv \eta_0 - \eta$.

Exercise 10.18 Show that, using the recurrence relation (Abramowitz and Stegun 1972):

$$\frac{j_{\ell}(x)}{x} = \frac{j_{\ell-1}(x) + j_{\ell+1}(x)}{2\ell+1} , \tag{10.229}$$

we can write:

$$a^T_{T,\ell m} = -i^{\ell} \sqrt{\frac{(2\ell+1)(\ell+2)!}{8\pi(\ell-2)!}} \sum_{\lambda=\pm 2} \int \frac{d^3\mathbf{k}}{(2\pi)^3} D^{(\ell)}_{m,\lambda}[R(\hat{k})]\beta(\mathbf{k}, \lambda) \int_0^{\eta_0} d\eta \; S^T(\eta, k) \frac{j_{\ell}(kr)}{(kr)^2} . \tag{10.230}$$

The Wigner D-matrix can be related to the spin-weighted spherical harmonics as follows:

$$D^{(\ell)}_{m,\pm 2}(\hat{k}) = \sqrt{\frac{4\pi}{2\ell+1}} {}_{\pm 2}Y^{-m}_{\ell}(\hat{k}) = \sqrt{\frac{4\pi}{2\ell+1}} {}_{\mp 2}Y^{m*}_{\ell}(\hat{k}) , \tag{10.231}$$

so we have:

$$\boxed{a^T_{T,\ell m} = -i^\ell \sqrt{\frac{(\ell+2)!}{2(\ell-2)!}} \sum_{\lambda=\pm 2} \int \frac{d^3\mathbf{k}}{(2\pi)^3} {}_\lambda Y^{m*}_\ell(\hat{k}) \beta(\mathbf{k}, \lambda) \int_0^{\eta_0} d\eta \; S^T(\eta, k) \frac{j_\ell(kr)}{(kr)^2}} \tag{10.232}$$

This is our main result of this section. It is not surprising that $Y^{m*}_\ell(\hat{k})$ eventually appeared, being GW a spin-2 field.

In order to compute the tensor contribution to the $C_{TT,\ell}$'s, we perform the ensemble average:

$$\langle a^T_{T,\ell m} a^{T*}_{T,\ell' m'} \rangle = C^T_{TT,\ell} \delta_{\ell\ell'} \delta_{mm'} \; . \tag{10.233}$$

Exercise 10.19 Assuming Gaussian perturbations, using Eq. (7.102) and the orthogonality property of the Wigner D-matrices or the spin-weighted spherical harmonics:

$$\int d^2\hat{k} \; D^{(\ell)}_{m,\pm 2}[R(\hat{k})] D^{(\ell')*}_{m',\pm 2}[R(\hat{k})] = \frac{4\pi}{2\ell+1} \delta_{\ell\ell'} \delta_{mm'} \; , \tag{10.234}$$

show that:

$$\boxed{C^T_{TT,\ell} = \frac{(\ell+2)!}{4\pi(\ell-2)!} \int_0^\infty \frac{dk}{k} \Delta^2_h(k) \left| \int_0^{\eta_0} d\eta \; S^T(\eta, k) \frac{j_\ell(kr)}{(kr)^2} \right|^2} \tag{10.235}$$

Note that a factor 2 arises because of the two polarisation states.

The above result was originally obtained in Abbott and Wise (1984) (though not exactly in the same way and final form).

The main difficulty we faced in computing the $a^T_{T,\ell m}$ was the spatial rotation which brought $\hat{k}$ in a generic direction. This can be avoided if we calculate straightaway $C^T_{TT,\ell}$ because it is rotationally invariant. Note that no correlation exists between scalar and tensor modes. In fact if we compute:

$$\langle a^T_{T,\ell m} a^{S*}_{T,\ell' m'} \rangle \; , \tag{10.236}$$

we would get zero, mathematically because of the integral:

$$\int d^2\hat{k} \; {}_2Y^m_\ell(\hat{k}) Y^{m'}_{\ell'}(\hat{k}) = 0 \; , \tag{10.237}$$

between a spin-2 spherical harmonic and a spin-0 one. Physically, because we know that at the linear order scalar and tensor perturbations do not couple.

We can again approximate this angular power spectrum for large values of ℓ as follows. First, $S^T(\eta, k)$ contains the derivative of h, which is maximum when a mode enters the horizon, for $k\eta \approx 1$, being almost zero elsewhere. Therefore, assuming instantaneous recombination, we can write:

$$C^T_{TT,\ell} = \frac{(\ell-1)\ell(\ell+1)(\ell+2)}{4\pi} \int_0^\infty \frac{dk}{k} \Delta^2_h(k) \frac{j^2_\ell(k\eta_0)}{(k\eta_0)^4} \,. \tag{10.238}$$

Defining the new variable $x \equiv k\eta_0$ and introducing the primordial tensor power spectrum we get:

$$C^T_{TT,\ell} \propto \frac{(\ell-1)\ell(\ell+1)(\ell+2)}{4\pi} \int_0^\infty dx\, x^{n_T-5} j^2_\ell(x) \,. \tag{10.239}$$

The integral can be performed exactly:

$$\int_0^\infty dx\, x^{n_T-5} = \frac{\sqrt{\pi}}{2} \frac{\Gamma[1-(n_T-4)/2]\Gamma[(n_T-4)/2+\ell]}{(4-n_T)\Gamma[1/2-(n_T-4)/2]\Gamma[\ell+2-(n_T-4)/2]} \,, \tag{10.240}$$

but in the case of $n_T = 0$, a scale-invariant primordial tensor spectrum, we get:

$$\frac{\ell(\ell+1)C^T_{TT,\ell}}{2\pi} \propto \frac{\ell(\ell+1)}{(\ell-2)(\ell+3)} \,. \tag{10.241}$$

The behaviour of the tensor contribution to the TT power spectrum is thus very different from the one coming from scalar perturbations. In Figs. 10.12 and 10.13 we display the numerical calculations done with CLASS of the total (solid line), scalar (dashed line) and tensor (dotted line) angular power spectra.

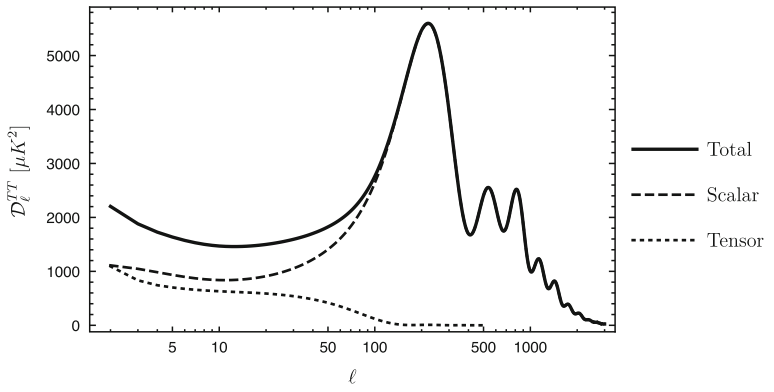

Fig. 10.12 Numerical calculations done with CLASS of the total (solid line), scalar (dashed line) and tensor (dotted line) angular power spectra

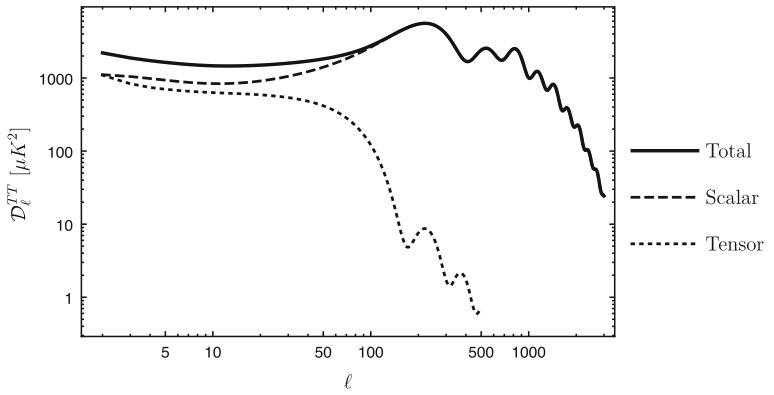

Fig. 10.13 Same as Fig. 10.12 but using a logarithmic scale

The tensor contribution is practically irrelevant on very small angular scale (i.e. large ℓ) and on large angular scales they can be as large as 10% of the total. Typically then one can give upper limits on $C^T_{TT,\ell}/C^S_{TT,\ell}$ for small multipoles ($\ell = 2$ or $\ell = 10$) and this ratio is proportional to A_T/A_S and therefore on the parameter r, the tensor-to-scalar ratio. From Eq. (8.176) we saw that $r < 0.1$. In order to determine this constraint one has also to use polarisation data since with these we are able to disentangle the $A_S \exp(-2\tau_{\rm reion})$ dependence coming from the scalar contribution only to the temperature power spectrum.

10.9 Polarisation

In this section we address CMB polarisation. Recall that before recombination polarisation is also erased because of tight-coupling. Polarisation is generated thanks to the fact that recombination does not take place instantaneously, so the finite-thickness effect is indeed important. Moreover, since Thomson scattering is axially-symmetric, circular polarisation is not produced.

In Sect. 12.7 we recall the main terminology regarding polarisation and in particular the Stokes parameters.

10.9.1 Scalar Perturbations Contribution to Polarisation

Now, let us focus on scalar perturbations only and write down from Eq. (5.115) the line of sight solution for the combination $Q + iU$. Since we have chosen a reference frame in which $\hat{k} = \hat{z}$, there is no U polarisation. This can be also seen from the fact that $\mathcal{B}^0 = 0$. Hence, we shall again perform a rotation in order to compute the $a_{P,\ell m}$.

We have called Θ_P the Stokes parameter Q in the $\hat{k} = \hat{z}$ frame. So, let us work on its line-of-sight solution.

Exercise 10.20 Show that:

$$\Theta_P(k\hat{z}, \hat{n}) = \frac{3}{2}\sqrt{\frac{8\pi}{15}}\,{}_2Y_2^0(\hat{n}) \int_0^{\eta_0} d\eta\, e^{-i\mu kr} S_P^S(\eta, k)\ , \tag{10.242}$$

where we have defined a new source term:

$$S_P^S(\eta, k) \equiv g(\eta)\Pi(\eta, k)\ . \tag{10.243}$$

We could have written ${}_{-2}Y_2^0(\hat{n})$ instead of ${}_2Y_2^0(\hat{n})$, since they are equal. However, we are going to deal with $Q + iU$ first. The above equation can written as:

$$\Theta_P(k\hat{z}, \hat{n}) = \sqrt{\frac{9}{30}}\,{}_2Y_2^0(\hat{p}) \sum_L i^L \sqrt{2L+1}\, Y_L^0(\hat{n}) \int_0^{\eta_0} d\eta\ S_P^S(\eta, k)\, j_L(kr)\ , \tag{10.244}$$

where again $r \equiv \eta_0 - \eta$ and we have used the well-known-by-now expansion of a plane wave into spherical harmonics plus the fact that $\hat{k} = \hat{z}$.

Now, as in Eq. (10.218) we can write the product of spherical harmonics as follows:

$$\begin{aligned} {}_2Y_2^0(\hat{n}) Y_L^0(\hat{n}) = \sqrt{\frac{5(2L+1)}{4\pi}} \sum_{L'} \sqrt{2L'+1} \\ \begin{pmatrix} L & 2 & L' \\ 0 & -2 & +2 \end{pmatrix} \begin{pmatrix} L & 2 & L' \\ 0 & 0 & 0 \end{pmatrix} {}_2Y_{L'}^0(\hat{n})\ , \end{aligned} \tag{10.245}$$

and thus obtain:

$$\begin{aligned} (Q + iU)^S(\hat{n}) = \sqrt{\frac{3}{8\pi}} \sum_L i^L (2L+1) \sum_{L'} \sqrt{2L'+1} \begin{pmatrix} L & 2 & L' \\ 0 & -2 & 2 \end{pmatrix} \\ \begin{pmatrix} L & 2 & L' \\ 0 & 0 & 0 \end{pmatrix} \sum_{m'} {}_2Y_{L'}^{m'}(\hat{n}) \int \frac{d^3\mathbf{k}}{(2\pi)^3} D_{m'0}^{(L')}(\hat{k}) \alpha(\mathbf{k}) \int_0^{\eta_0} d\eta\ S_P^S(\eta, k)\, j_L(kr)\ , \end{aligned} \tag{10.246}$$

where we have already considered the rotation which brings $\hat{k}$ in a generic direction.

Now, from the expansion:

$$(Q + iU)^S(\hat{n}) = \sum_{\ell m} a_{P,\ell m}^S\ {}_2Y_\ell^m(\hat{n})\ , \tag{10.247}$$

we are able to calculate the coefficients $a^S_{P,\ell m}$ by taking advantage of the orthonormality of the spin-2 spherical harmonics. We can therefore write:

$$a^S_{P,\ell m} = \sqrt{\frac{3}{8\pi}} \sum_L i^L (2L+1)\sqrt{2\ell+1} \begin{pmatrix} L & 2 & \ell \\ 0 & -2 & 2 \end{pmatrix} \begin{pmatrix} L & 2 & \ell \\ 0 & 0 & 0 \end{pmatrix} \int \frac{d^3\mathbf{k}}{(2\pi)^3} D^{(\ell)}_{m0}(\hat{k}) \alpha(\mathbf{k}) \int_0^{\eta_0} d\eta \; S^S_P(\eta, k) j_L(kr) \; . \tag{10.248}$$

Remarkably, the sum over L can be performed in the very same way we did for the $a^T_{T,\ell m}$, since the $3j$ symbols are the same. Therefore, we have:

$$a^S_{P,\ell m} = -\frac{3i^\ell}{8} \sqrt{\frac{(2\ell+1)(\ell+2)!}{\pi(\ell-2)!}} \int \frac{d^3\mathbf{k}}{(2\pi)^3} D^{(\ell)}_{m0}(\hat{k}) \alpha(\mathbf{k}) \int_0^{\eta_0} d\eta \; S^S_P(\eta, k) \frac{j_\ell(kr)}{(kr)^2} \; , \tag{10.249}$$

and using

$$D^{(\ell)}_{m0}(\hat{k}) = \sqrt{\frac{4\pi}{2\ell+1}} Y^{-m}_\ell(\hat{k}) = \sqrt{\frac{4\pi}{2\ell+1}} Y^{m*}_\ell(\hat{k}) \; , \tag{10.250}$$

we can write:

$$\boxed{a^S_{P,\ell m} = -\frac{3i^\ell}{4} \sqrt{\frac{(\ell+2)!}{(\ell-2)!}} \int \frac{d^3\mathbf{k}}{(2\pi)^3} Y^{m*}_\ell(\hat{k}) \alpha(\mathbf{k}) \int_0^{\eta_0} d\eta \; S^S_P(\eta, k) \frac{j_\ell(kr)}{(kr)^2}} \tag{10.251}$$

The expansion for $(Q - iU)^S(\hat{n})$ can be obtained by complex conjugation, i.e.

$$(Q - iU)(\hat{n}) = \sum_{\ell m} a^*_{P,\ell m} \; {}_2Y^{m*}_\ell(\hat{n}) = \sum_{\ell m} a^*_{P,\ell m} \; {}_{-2}Y^{-m}_\ell(\hat{n}) = \sum_{\ell m} a^*_{P,\ell,-m} \; {}_{-2}Y^{m}_\ell(\hat{n}) \; . \tag{10.252}$$

There is no reality condition here holding true for the $a_{P,\ell m}$ as the one holding true for the $a_{T,\ell m}$, because $Q + iU$ is not real and is not a scalar. It is thus convenient to define the following combinations:

$$a_{E,\ell m} \equiv -(a_{P,\ell m} + a^*_{P,\ell,-m})/2 \; , \quad a_{B,\ell m} \equiv i(a_{P,\ell m} - a^*_{P,\ell,-m})/2 \; , \tag{10.253}$$

because the first has parity $(-1)^\ell$ whereas the second $(-1)^{\ell+1}$. Thus $Q \pm iU$ can be expanded as:

$$(Q \pm iU)(\hat{n}) = \sum_{\ell m} (-a_{E,\ell m} \mp i a_{B,\ell m})\, {}_2Y_\ell^m(\hat{n}) \,. \tag{10.254}$$

Now, if we compute $a^{S*}_{P,\ell m}$, we obtain:

$$a^{S*}_{P,\ell m} = -\frac{3(-i)^\ell}{4}\sqrt{\frac{(\ell+2)!}{(\ell-2)!}} \int \frac{d^3\mathbf{k}}{(2\pi)^3} Y_\ell^{-m*}(\hat{k})\alpha(-\mathbf{k}) \int_0^{\eta_0} d\eta\; S^S_P(\eta,k)\frac{j_\ell(kr)}{(kr)^2} \,, \tag{10.255}$$

since $\alpha(\mathbf{k})^* = \alpha(-\mathbf{k})$ because of the reality condition of the power spectrum. Changing the integration variable to $\mathbf{k}$ and using the parity of the spherical harmonic:

$$Y_\ell^{-m*}(-\hat{k}) = (-1)^\ell Y_\ell^{-m*}(\hat{k}) \,, \tag{10.256}$$

we can finally conclude that:

$$a^S_{P,\ell m} = a^{S*}_{P,\ell,-m} \,, \tag{10.257}$$

and therefore scalar perturbations only affect the E-mode, i.e.

$$a^S_{E,\ell m} = -a^S_{P,\ell m} \,, \qquad a^S_{B,\ell m} = 0 \,. \tag{10.258}$$

This means that, if the B-mode was detected, it would be a clear indication of the existence of primordial gravitational waves.

From Eq. (10.251) we can then obtain the scalar contribution to the EE spectrum. Assuming adiabatic Gaussian perturbations:

$$\boxed{C^S_{EE,\ell} = \frac{9}{64\pi}\frac{(\ell+2)!}{(\ell-2)!}\int \frac{dk}{k}\Delta^2_{\mathcal{R}} \left| \int_0^{\eta_0} d\eta\; S^S_P(\eta,k)\frac{j_\ell(kr)}{(kr)^2}\right|^2} \tag{10.259}$$

Using instead Eq. (10.176) we can compute the cross-correlation TE multipole coefficients:

$$\boxed{C^S_{TE,\ell} = -\frac{3}{4}\sqrt{\frac{(\ell+2)!}{(\ell-2)!}}\int \frac{dk}{k}\Delta^2_{\mathcal{R}}\Theta_\ell(k) \int_0^{\eta_0} d\eta\; S^S_P(\eta,k)\frac{j_\ell(kr)}{(kr)^2}} \tag{10.260}$$

10.9.2 Tensor Perturbations Contribution to Polarisation

Let us now calculate the contribution to CMB polarisation coming from tensor perturbations. From Eq. (10.211) we have

$$\Theta_P^{(T)}(\eta_0, k\hat{z}, \mu) = \int_0^{\eta_0} d\eta \, e^{ik\mu(\eta-\eta_0)} S_P^T(\eta, k) \, , \tag{10.261}$$

with

$$S_P^T(\eta, k) \equiv g(\eta)\mathcal{S}^T(\eta, k) \, . \tag{10.262}$$

and then use Eq. (5.132) in order to write part of the tensor contribution to polarization:

$$\mathcal{Q}_\lambda^{(T)}(k\hat{z}, \hat{p}) \equiv \sqrt{\frac{8\pi}{5}} \mathcal{E}^\lambda(\hat{p}) \int_0^{\eta_0} d\eta \, e^{-i\mu k r(\eta)} S_P^T(\eta, k) \, , \tag{10.263}$$

where $r(\eta) \equiv \eta_0 - \eta$ and where we stress that the result holds true for $\hat{k} = \hat{z}$ since this was the condition under which we derived the Boltzmann equation for photons.

In the scalar case no U contribution to polarisation is produced, so the above expression already furnishes the quantity $Q + iU$. However, the same is not true for tensor perturbation. We have thus to add the iU contribution. As we saw in Chap. 5 this is equal to $\mathcal{B}^m Q/\mathcal{E}^m$ and for this reason we have just one polarisation hierarchy. Hence, summing up we get:

$$(\mathcal{Q}_\lambda + i\mathcal{U}_\lambda)^{(T)}(k\hat{z}, \hat{n}) = \sqrt{\frac{32\pi}{5}} {}_2Y_2^\lambda(\hat{n}) \int_0^{\eta_0} d\eta \, e^{i\hat{k}\cdot\hat{n} k r(\eta)} S_P^T(\eta, k) \, . \tag{10.264}$$

Using the usual plane-wave expansion and recalling that $\hat{k} = \hat{z}$ we get:

$$(\mathcal{Q}_\lambda + i\mathcal{U}_\lambda)^{(T)}(k\hat{z}, \hat{n}) = \sqrt{\frac{8}{5}} {}_2Y_2^\lambda(\hat{n}) \sum_L i^L \sqrt{2L+1} Y_L^0(\hat{n}) \int_0^{\eta_0} d\eta \, S_P^T(\eta, k) j_L(kr) \, . \tag{10.265}$$

The product of the two spherical harmonics can be written via the Wigner $3j$-symbols as follows:

$${}_2Y_2^{\pm 2}(\hat{n}) Y_L^0(\hat{n}) = \sqrt{\frac{5(2L+1)}{4\pi}} \sum_{L'} \sqrt{2L'+1} \begin{pmatrix} L & 2 & L' \\ 0 & \pm 2 & \mp 2 \end{pmatrix} \begin{pmatrix} L & 2 & L' \\ 0 & -2 & 2 \end{pmatrix} {}_2Y_{L'}^{\pm 2}(\hat{n}) \, , \tag{10.266}$$

and we rotate in a generic $\hat{k}$ direction the only spherical harmonic left, i.e.

$${}_2Y_{L'}^{\pm 2}(R\hat{n}) = \sum_{m'=-L'}^{L'} D_{m',\pm 2}^{(L')}[R^{-1}(\hat{k})] {}_2Y_{L'}^{m'}(\hat{n}) \, . \tag{10.267}$$

Hence, we can write:

$$(\mathcal{Q}_\lambda + i\mathcal{U}_\lambda)^{(T)}(\mathbf{k},\hat{n}) = \sqrt{\frac{2}{\pi}}\sum_L i^L(2L+1)\sum_{L'}\sqrt{2L'+1}\begin{pmatrix} L & 2 & L' \\ 0 & \lambda & -\lambda \end{pmatrix}$$
$$\begin{pmatrix} L & 2 & L' \\ 0 & -2 & 2 \end{pmatrix}\sum_{m'} D^{(L')}_{m'\lambda}[R(\hat{k})]Y^{m'}_{L'}(\hat{n})\int_0^{\eta_0} d\eta\; S^T_P(\eta,k)j_L(kr)\;. \quad (10.268)$$

Now we can perform the Fourier anti-transform. Multiply by $\beta(\mathbf{k},\lambda)$ and ${}_2Y^{m*}_\ell(\hat{n})$ and integrate over $d^2\hat{n}$ in order to obtain the $a^T_{P,\ell m}$'s. We obtain:

$$a^T_{P,\ell m,\pm 2} = \sqrt{\frac{2}{\pi}}\sum_L i^L(2L+1)\sqrt{2\ell+1}\begin{pmatrix} L & 2 & \ell \\ 0 & \pm 2 & \mp 2 \end{pmatrix}$$
$$\begin{pmatrix} L & 2 & \ell \\ 0 & -2 & 2 \end{pmatrix}\int \frac{d^3\mathbf{k}}{(2\pi)^3} D^{(\ell)}_{m\pm 2}[R(\hat{k})]\beta(\mathbf{k},\lambda)\int_0^{\eta_0} d\eta\; S^T_P(\eta,k)j_L(kr)\;. \quad (10.269)$$

We have used here the orthonormality relation of the spin-2 spherical harmonics and distinguished the contributions of different helicity. Of course $a^T_{P,\ell m} = a^T_{P,\ell m,+2} + a^T_{P,\ell m,-2}$.

We have already computed some of the $3j$ symbols earlier, for the tensor case but now two more enter: those for $L = \ell \pm 1$. We shall see that these contributions will characterise the B-mode of polarisation. They are:

$$\begin{pmatrix} \ell+1 & \ell & 2 \\ 0 & -2 & +2 \end{pmatrix} = (-1)^{\ell+1}\sqrt{\frac{(\ell-1)}{2(2\ell+1)(2\ell+3)}}\;, \quad (10.270)$$

$$\begin{pmatrix} \ell & \ell-1 & 2 \\ -2 & 0 & +2 \end{pmatrix} = (-1)^{\ell}\sqrt{\frac{(\ell+2)}{2(2\ell-1)(2\ell+1)}}\;. \quad (10.271)$$

Extra care has to be used when manipulating these terms. The reason is that the $3j$ symbols gain an overall phase factor

$$(-1)^{j_1+j_2+j_3}\;, \quad (10.272)$$

where $j_{1,2,3}$ are the momenta which are being combined, each time we swap two columns or change simultaneously all the signs of the bottom row.[4] Therefore, as long as $j_1 + j_2 + j_3$ is even, no matter how many times we perform the above operations. This is the case for $L = \ell \pm 2$ or $L = \ell$. However, for $L = \ell \pm 1$ we have that

[4] These signs can be changed only simultaneously since the sums $m_1 + m_2 + m_3 = 0$ always. This is a selection rule.

$$L + \ell + 2 = 2(\ell + 1) \pm 1 \,, \tag{10.273}$$

which is odd and thus we have to keep track of the correct sign.

Exercise 10.21 Using the formulas for the $3j$ symbols, show that:

$$a^T_{P,\ell m,\pm 2} = \frac{-i^\ell \sqrt{2\ell+1}}{\sqrt{8\pi}} \int \frac{d^3\mathbf{k}}{(2\pi)^3} D^{(\ell)}_{m\pm 2}[R(\hat{k})]\beta(\mathbf{k},\lambda) \int_0^{\eta_0} d\eta \; S^T_P(\eta,k)$$
$$\left[\frac{(\ell+1)(\ell+2)}{(2\ell-1)(2\ell+1)} j_{\ell-2}(kr) - \frac{6(\ell-1)(\ell+2)}{(2\ell-1)(2\ell+3)} j_\ell(kr) + \frac{(\ell-1)\ell}{(2\ell+1)(2\ell+3)} j_{\ell+2}(kr) \right.$$
$$\left. \pm 2i \frac{\ell-1}{2\ell+1} j_{\ell+1}(kr) \mp 2i \frac{\ell+2}{2\ell+1} j_{\ell-1}(kr) \right] . \tag{10.274}$$

Recall that $r = r(\eta) \equiv \eta_0 - \eta$.

Exercise 10.22 Show that, using the recurrence relation of Eq. (10.229) and the following ones for the derivatives:

$$j'_\ell(x) = j_{\ell-1}(x) - \frac{\ell+1}{x} j_\ell(x) \,, \quad j'_\ell(x) = \frac{\ell}{x} j_\ell(x) - j_{\ell+1}(x) \,, \tag{10.275}$$

we can write:

$$a^T_{P,\ell m} = \frac{-i^\ell \sqrt{2\ell+1}}{\sqrt{8\pi}} \sum_{\lambda=\pm 2} \int \frac{d^3\mathbf{k}}{(2\pi)^3} D^{(\ell)}_{m,\lambda}[R(\hat{k})]\beta(\mathbf{k},\lambda) \int_0^{\eta_0} d\eta \; S^T_P(\eta,k)$$
$$\left[\frac{2}{kr} j'_\ell - 2 j_\ell + \frac{2 + \ell(\ell+1)}{(kr)^2} j_\ell - i\lambda \left(j'_\ell + \frac{2}{kr} j_\ell \right) \right] . \tag{10.276}$$

Show that the term between square brackets is equal to the corresponding one in Weinberg (2008, p. 389). In order to make the second derivative of the spherical Bessel function to appear one must use Bessel differential equation:

$$j''_\ell + \frac{2}{x} j_\ell + \frac{1 - \ell(\ell+1)}{x^2} j_\ell = 0 \,. \tag{10.277}$$

Now we are ready to investigate the reality property of $a^T_{P,\ell m}$ and discern from it the E-mode and B-mode contributions. Recall that Wigner D-matrix can be related to the spin-weighted spherical harmonics as follows:

$$D^{(\ell)}_{m,\pm 2}(\hat{k}) = \sqrt{\frac{4\pi}{2\ell+1}}\,{}_{\pm 2}Y^{-m}_{\ell}(\hat{k}) = \sqrt{\frac{4\pi}{2\ell+1}}\,{}_{\mp 2}Y^{m*}_{\ell}(\hat{k})\,. \tag{10.278}$$

So taking the complex conjugate we find:

$$a^{T*}_{P,\ell m} = -\frac{(-i)^{\ell}}{\sqrt{2}}\sum_{\lambda=\pm 2}\int \frac{d^3\mathbf{k}}{(2\pi)^3}\,{}_{\mp 2}Y^{m}_{\ell}(\hat{k})\beta(-\mathbf{k},\lambda)\int_0^{\eta_0} d\eta\; S^T_P(\eta,k) \left[\frac{2}{kr}j'_{\ell} - 2j_{\ell} + \frac{2+\ell(\ell+1)}{(kr)^2}j_{\ell} + i\lambda\left(j'_{\ell}+\frac{2}{kr}j_{\ell}\right)\right]. \tag{10.279}$$

Note that $\beta(\mathbf{k},\lambda)* = \beta(-\mathbf{k},\lambda)$ because of the reality condition and beware that the sign of the imaginary unit inside the square brackets has changed. Now, changing integration variable

$$\mathbf{k} \to -\mathbf{k}\,, \tag{10.280}$$

and taking advantage of the parity property and the complex conjugation property:

$${}_{\mp 2}Y^{m}_{\ell}(-\hat{k}) = (-1)^{\ell}\,{}_{\pm 2}Y^{m}_{\ell}(\hat{k}) = (-1)^{\ell}\,{}_{\mp 2}Y^{-m*}_{\ell}(\hat{k})\,, \tag{10.281}$$

we get:

$$a^{T*}_{P,\ell m} = -\frac{i^{\ell}}{\sqrt{2}}\sum_{\lambda=\pm 2}\int \frac{d^3\mathbf{k}}{(2\pi)^3}\,{}_{\mp 2}Y^{-m*}_{\ell}(\hat{k})\beta(\mathbf{k},\lambda)\int_0^{\eta_0} d\eta\; S^T_P(\eta,k) \left[\frac{2}{kr}j'_{\ell} - 2j_{\ell} + \frac{2+\ell(\ell+1)}{(kr)^2}j_{\ell} + i\lambda\left(j'_{\ell}+\frac{2}{kr}j_{\ell}\right)\right]. \tag{10.282}$$

This time we have not the same situation as in Eq. (10.257) because of the $i\lambda$ contribution. Hence, we can compute the E-mode:

$$a^{T}_{E,\ell m} = \frac{i^{\ell}}{\sqrt{2}}\sum_{\lambda=\pm 2}\int \frac{d^3\mathbf{k}}{(2\pi)^3}\,{}_{\mp 2}Y^{m*}_{\ell}(\hat{k})\beta(\mathbf{k},\lambda)\int_0^{\eta_0} d\eta\; S^T_P(\eta,k) \left[\frac{2}{kr}j'_{\ell} - 2j_{\ell} + \frac{2+\ell(\ell+1)}{(kr)^2}j_{\ell}\right]. \tag{10.283}$$

and the B-mode is also present:

$$\boxed{a^{T}_{B,\ell m} = -\frac{i^{\ell}}{\sqrt{2}}\sum_{\lambda=\pm 2}\lambda\int \frac{d^3\mathbf{k}}{(2\pi)^3}\,{}_{\mp 2}Y^{m*}_{\ell}(\hat{k})\beta(\mathbf{k},\lambda)\int_0^{\eta_0} d\eta\; S^T_P(\eta,k)\left(j'_{\ell}+\frac{2}{kr}j_{\ell}\right)} \tag{10.284}$$

Now we are in position of giving the formulas for the angular power spectra. Assuming Gaussian perturbations we have:

$$C^T_{EE,\ell} = \int \frac{dk}{4\pi k} \Delta^2_h(k) \left| \int_0^{\eta_0} d\eta \; S^T_P(\eta, k) \left[\frac{2}{kr} j'_\ell - 2 j_\ell + \frac{2 + \ell(\ell+1)}{(kr)^2} j_\ell \right] \right|^2 , \tag{10.285}$$

and

$$C^T_{BB,\ell} = \int \frac{dk}{4\pi k} \Delta^2_h \left| \int_0^{\eta_0} d\eta \; S^T_P(\eta, k) \left(2 j'_\ell + \frac{4}{kr} j_\ell \right) \right|^2 . \tag{10.286}$$

The cross-correlation $C^T_{TE,\ell}$, using Eq. (10.232) gives:

$$C^T_{TE,\ell} = -\sqrt{\frac{(\ell+2)!}{(\ell-2)!}} \int \frac{dk}{8\pi k} \Delta^2_h(k) \int_0^{\eta_0} d\eta \; S^T(\eta, k) \frac{j_\ell}{(kr)^2} \int_0^{\eta_0} d\eta' S^T_P(\eta', k) \left[\frac{2}{kr} j'_\ell - 2 j_\ell + \frac{2 + \ell(\ell+1)}{(kr)^2} j_\ell \right] . \tag{10.287}$$

If we try to compute the cross correlations $C^T_{TB,\ell}$ and $C^T_{EB,\ell}$ we obtain a vanishing result, as expected, because of the term λ in the sum of Eq. (10.284). In fact we get, considering for example $C^T_{EB,\ell}$:

$$C^T_{EB,\ell} = -\sum_{\lambda=\pm 2} \frac{\lambda}{2} \int \frac{dk}{4\pi k} \Delta^2_h \int_0^{\eta_0} d\eta \; S^T_P(\eta, k) \left[\frac{2}{kr} j'_\ell - 2 j_\ell + \frac{2 + \ell(\ell+1)}{(kr)^2} j_\ell \right] \int_0^{\eta_0} d\bar{\eta} \; S^T_P(\bar{\eta}, k) \left(2 j'_\ell + \frac{4}{kr} j_\ell \right) . \tag{10.288}$$

Now, the sum over λ is equivalent to a difference and since nothing else depends on λ the result is zero. The same happens with the correlation $C^T_{TB,\ell}$.

In Fig. 10.14 we display the 4 angular CMB power spectra which constitute a wealth of cosmological information. The only possible cross-correlation is the one between temperature and the E-mode of polarisation. The largest signal is the TT one and then, in order of decreasing power, the TE, EE and BB one. The latter is 5 orders of magnitude smaller than the TT one and it has not yet been detected. The bump it displays for small ℓ's is due to reionisation.

From Fig. 10.14 we can appreciate how small the polarisation spectra are with respect to the TT one. This is due to the fact that a quadrupole moment in the distribution of photons is needed in order to have production of polarisation. Before recombination, Thomson scattering rate is so high that photons are in nearly perfect

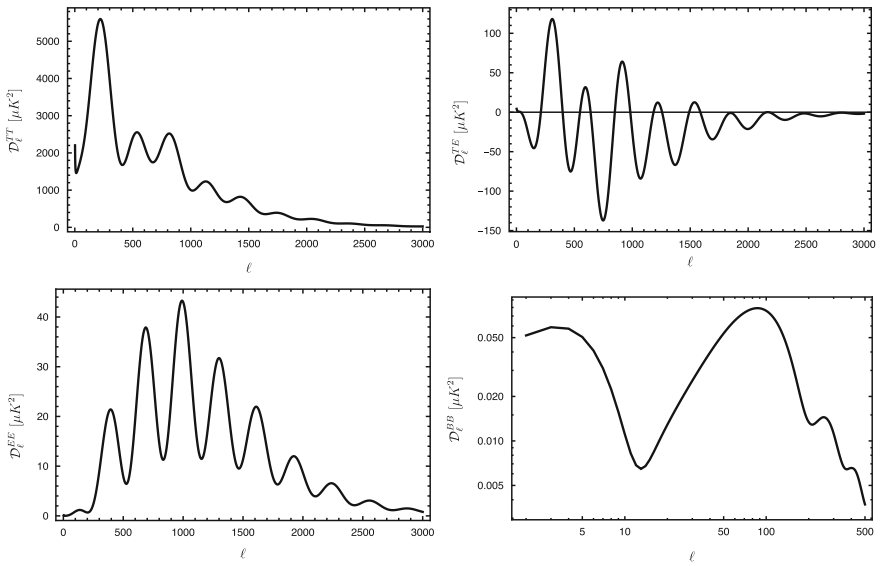

Fig. 10.14 The four angular power spectra characterising the CMB, computed with CLASS for the standard model. Top left: TT. Top right: TE. Bottom left: EE. Bottom right: BB. As for the TT spectrum, $\mathcal{D} \equiv \ell(\ell+1)C_\ell/(2\pi)$

thermal equilibrium and any moment from the quadrupole up is washed out. After recombination, photons free stream and thus have no more chance of being polarised by Thomson scattering.

References

Abbott, L.F., Wise, M.B.: Constraints on generalized inflationary cosmologies. Nucl. Phys. B **244**, 541–548 (1984)

Abramowitz, M., Stegun, I.A.: Handbook of Mathematical Functions With Formulas, Graphs, and Mathematical Tables. Dover (1972)

Ade, P.A.R., et al.: Planck 2015 results. XIII. Cosmological parameters. Astron. Astrophys. **594**, A13 (2016)

Eisenstein, D.J., et al.: Detection of the baryon acoustic peak in the large-scale correlation function of SDSS luminous red galaxies. Astrophys. J. **633**, 560–574 (2005)

Hu, W., Sugiyama, N.: Small scale cosmological perturbations: an analytic approach. Astrophys. J. **471**, 542–570 (1996)

Kaiser, N.: Small-angle anisotropy of the microwave background radiation in the adiabatic theory. MNRAS **202**, 1169–1180 (1983)

Landau, L.D., Lifshits, E.M.: Quantum Mechanics. Volume 3 of Course of Theoretical Physics. Butterworth-Heinemann, Oxford (1991)

Ma, C.-P., Bertschinger, E.: Cosmological perturbation theory in the synchronous and conformal Newtonian gauges. Astrophys. J. **455**, 7–25 (1995)

Mukhanov, V.F.: CMB-slow, or how to estimate cosmological parameters by hand. Int. J. Theor. Phys. **43**, 623–668 (2004)
Mukhanov, V.: Physical Foundations of Cosmology. Cambridge University Press, Cambridge (2005)
Racah, G.: Theory of complex spectra. II. Phys. Rev. **62**(9–10), 438 (1942)
Sachs, R.K., Wolfe, A.M.: Perturbations of a cosmological model and angular variations of the microwave background. Astrophys. J. **147**, 73–90 (1967)
Seljak, U., Zaldarriaga, M.: A line of sight integration approach to cosmic microwave background anisotropies. Astrophys. J. **469**, 437–444 (1996)
Silk, J.: Fluctuations in the primordial fireball. Nature **215**(5106), 1155–1156 (1967)
Wands, D., Piattella, O.F., Casarini, L.: Physics of the cosmic microwave background radiation. Astrophys. Space Sci. Proc. **45**, 3–39 (2016)
Weinberg, S.: Cosmology. Oxford University Press, Oxford (2008)
Weinberg, S.: Lectures on Quantum Mechanics. Cambridge University Press, Cambridge (2015)